AD-A061 085 NATIONAL SEVERE STORMS LAB NORMAN OKLA F/G 17/9
ECHO INTERPRETATION OF SEVERE STORMS ON AIRPORT SURVEILLANCE RA--ETC(U)
APR 78 W D ZITTEL DOT-FA77WAI-724
UNCLASSIFIED FAA/RD-78/60 NL

END
DATE FILMED
1-79
DDC

Report No. FAA-RD-78-60

LEVEL II

12 B.S.

DDC FILE COPY AD A061085

ECHO INTERPRETATION OF SEVERE STORMS ON AIRPORT SURVEILLANCE RADARS

W. David Zittel

National Severe Storms Laboratory
Environmental Research Laboratories
National Oceanic and Atmospheric Administration

DDC RECEIVED NOV 13 1978 F

April 1978

Phase I Report

Document is available to the U.S. public through the National Technical Information Service, Springfield, Virginia 22161.

Prepared for

U.S. DEPARTMENT OF TRANSPORTATION
FEDERAL AVIATION ADMINISTRATION
Systems Research & Development Service
Washington, D.C. 20590

78 11 09 033

NOTICE

This document is disseminated under the sponsorship of the Department of Transportation in the interest of information exchange. The United States Government assumes no liability for its contents or use thereof.

(18) FAA/RD (19) 78/60

Technical Report Documentation Page

1. Report No.	2. Government Accession No.	3. Recipient's Catalog No.
FAA-RD-78-60		

4. Title and Subtitle
(6) Echo Interpretation of Severe Storms on Airport Surveillance Radars

5. Report Date
(11) April 1978

6. Performing Organization Code

8. Performing Organization Report No.

7. Author(s)
(10) W. David Zittel

9. Performing Organization Name and Address
National Severe Storms Laboratory
Environmental Research Laboratories
National Oceanic and Atmospheric Administration

10. Work Unit No. (TRAIS)

11. Contract or Grant No.
DOT: FA77WAI-724 New

12. Sponsoring Agency Name and Address
Department of Transportation
Federal Aviation Administration
Systems Research and Development Service
Washington, D. C. 20590

(13) 71 p.

13. Type of Report and Period Covered
Phase I
Feb 15, 1977 to May 31, 1978

14. Sponsoring Agency Code
ARD-451

15. Supplementary Notes
(15) DOT-FA77WAI-724

16. Abstract

Past research indicates ASR radars have sufficient sensitivity to detect severe storms. This report provides background information about severe storm climatology and morphology and then considers the effects various ASR radar operational "fixes" have in identifying severe storms, based on current knowledge of storm structure.

Results show identification of severe storms with ASR radars is unlikely without accurate reflectivity displays and with the use of MTI and CP. Operationally, it is recommended that outside data sources provide initial severe storm identification, while the ASRs are used to supplement this data by giving storm positions in real time.

(9) Rept. for 15 Feb 77-31 May 78 on Phase 1,

17. Key Words	18. Distribution Statement
Severe Storms Airport Surveillance Radars	Document is available to the public through the National Technical Information Service, Springfield, VA. 22151.

19. Security Classif. (of this report)	20. Security Classif. (of this page)	21. No. of Pages	22. Price
Unclassified	Unclassified	69	

Form DOT F 1700.7 (8-72) Reproduction of completed page authorized

244 670

METRIC CONVERSION FACTORS

Approximate Conversions to Metric Measures

Symbol	When You Know	Multiply by	To Find	Symbol
	LENGTH			
in	inches	*2.5	centimeters	cm
ft	feet	30	centimeters	cm
yd	yards	0.9	meters	m
mi	miles	1.6	kilometers	km
	AREA			
in^2	square inches	6.5	square centimeters	cm^2
ft^2	square feet	0.09	square meters	m^2
yd^2	square yards	0.8	square meters	m^2
mi^2	square miles	2.6	square kilometers	km^2
	acres	0.4	hectares	ha
	MASS (weight)			
oz	ounces	28	grams	g
lb	pounds	0.45	kilograms	kg
	short tons (2000 lb)	0.9	tonnes	t
	VOLUME			
tsp	teaspoons	5	milliliters	ml
Tbsp	tablespoons	15	milliliters	ml
fl oz	fluid ounces	30	milliliters	ml
c	cups	0.24	liters	l
pt	pints	0.47	liters	l
qt	quarts	0.95	liters	l
gal	gallons	3.8	liters	l
ft^3	cubic feet	0.03	cubic meters	m^3
yd^3	cubic yards	0.76	cubic meters	m^3
	TEMPERATURE (exact)			
°F	Fahrenheit temperature	5/9 (after subtracting 32)	Celsius temperature	°C

*1 in. = 2.54 (exactly). For other exact conversions and more detailed tables, see NBS Misc. Publ. 286, *Units of Weights and Measures, Price $2.25, SD Catalog No. C13.10:286.*

Approximate Conversions from Metric Measures

Symbol	When You Know	Multiply by	To Find	Symbol
	LENGTH			
mm	millimeters	0.04	inches	in
cm	*centimeters*	0.4	inches	in
m	meters	3.3	feet	ft
m	meters	1.1	yards	yd
km	kilometers	0.6	miles	mi
	AREA			
cm^2	square centimeters	0.16	square inches	in^2
m^2	square meters	1.2	square yards	yd^2
km^2	square kilometers	0.4	square miles	mi^2
ha	hectares (10,000 m^2)	2.5	acres	
	MASS (weight)			
g	*grams*	0.035	ounces	oz
kg	kilograms	2.2	pounds	lb
t	tonnes (1000 kg)	1.1	short tons	
	VOLUME			
ml	milliliters	0.03	fluid ounces	fl oz
l	liters	2.1	pints	pt
l	liters	1.06	quarts	qt
l	liters	0.26	gallons	gal
m^3	cubic meters	35	cubic feet	ft^3
m^3	cubic meters	1.3	cubic yards	yd^3
	TEMPERATURE (exact)			
°C	Celsius temperature	9/5 (then add 32)	Fahrenheit temperature	°F

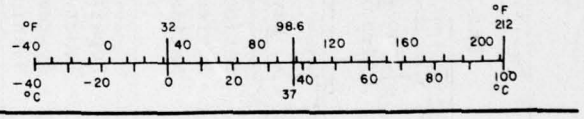

TABLE OF CONTENTS

ACCESSION for
NTIS White Section
DDC Buff Section
UNANNOUNCED
JUSTIFICATION
BY
DISTRIBUTION/AVAILABILITY CODES
Dist. SPECIAL

TABLE OF CONTENTS (cont.)

LIST OF FIGURES

LIST OF FIGURES (cont.)

LIST OF FIGURES (cont.)

LIST OF FIGURES (cont.)

LIST OF TABLES

LIST OF ABBREVIATIONS

ARTCC	Air Route Traffic Control Center
ASR	Airport Surveillance Radar
CFCF	Central Flow Control Facility
CP	Circular Polarization
Csc^2	Cosecant squared
FA	Flight Advisory
FAA	Federal Aviation Administration
FSS	Flight Service Station
FTC	Fast Time Constant
GMT	Greenwich Mean Time
IF	Intermediate Frequency
LEWP	Line Echo Wave Pattern
LP	Linear Polarization
MTI	Moving Target Indicator
NAFEC	National Aviation Facilities Experimental Center
NAMFAX	National and Aviation Meteorological Facsimile Circuit
NMC	National Meteorological Center
NSSFC	National Severe Storms Forecast Center
NWS	National Weather Service
NWSFO	National Weather Service Forecast Office
NWSO	National Weather Service Observatory
PIREP	Pilot Reports
PPI	Plan Position Indicator
PRF	Pulse Repetition Frequency

LIST OF ABBREVIATIONS (cont.)

RAREP	Radar Report
RAWARC	Rarep and Warning Coordination Teletype Circuit
SCV	Sub Clutter Visibility
SELS	Severe Local Storms Unit
SIGMET	Significant Meteorological Information Bulletin
STC	Sensitivity Time Control
TRACON	Terminal Radar Control
WMSC	Weather Message Switching Center
WSR	Weather Surveillance Radar

78 11 09 033

ECHO INTERPRETATION OF SEVERE STORMS ON AIRPORT SURVEILLANCE RADARS

W. David Zittel

1. INTRODUCTION

The Federal Aviation Administration (FAA) is sponsoring the development of new techniques and is considering deploying arrays of meteorological sensors to monitor severe storms and their related hazards more closely. Also receiving attention are methods and equipment to display these data remotely to air traffic controllers. For years, the FAA has operated radars which have enough sensitivity to detect severe storms (see, for example, Wilk et al., 1965). But selectable features are incorporated into these radars to attenuate weather display whenever it interferes with the detection and display of aircraft targets for air traffic control.

The goals, herein, are to describe weather conditions which foster severe storms; explain National Weather Service (NWS) forecasts, advisories and warnings; and review the limits and adaptations of FAA radars to show and identify severe storms accurately (to help the FAA judge use of manpower and equipment). Although FAA radars can detect severe storms, it may be advisable to provide more and faster communications between the NWS and FAA by remoting NWS radar data to controllers. And, finally, in order for any warning system to be effective, pilots must heed NWS and FAA advisories and warnings of probable hazards in and near severe thunderstorms and plan their flights accordingly. An important focus of this report is the problem air traffic controllers face in controlling aircraft for safe traffic separation while having incomplete knowledge of hazardous weather conditions which force flight plan deviations.

2. BACKGROUND INFORMATION ON SEVERE STORMS

2.1 Synoptic Weather Conditions

All substantial precipitation, whether ice or liquid, results from ascending moist air; the rate and distribution of ascent determines whether precipitation is heavy or light, irregular or continuous. Upward air motions in thunderstorms more than 60 kts (30 m sec^{-1}) have been observed, but motions in light precipitation of only a centimeter per second are common. The factors which determine the rate air ascends, and hence the kind of precipitation at any given place, are air mass stability, frontal positions and insolation. These factors are influenced heavily by latitude, terrain features, distribution of land and water, time of year, and time of day. This section discusses thunderstorm causes and storms' spatial and temporal distributions. A severe thunderstorm by NWS definition is: A thunderstorm which produces a tornado, hail three-quarter inch or larger on the ground, and/or winds greater than or equal to 50 kts (25 m sec^{-1}).

Vertical profiles of moisture, temperature, and wind must occur in certain patterns to cause severe thunderstorms. Abundant moisture must exist through a depth of at least 3000 ft (1 km) with surface dewpoint temperatures at 55°F or higher. Above this moist layer must be a layer of much drier air usually extending to the tropopause. The air temperature must decline rapidly with height so that air parcels from the warm moist lower levels will maintain their relative warmth, and hence buoyancy, as they rise. At the tropopause the air temperature ceases to decline rapidly with height. The tropopause varies in height with latitude, from 60,000 ft (20 km) at the equator in summer, to under 20,000 ft (7 km) at the poles in winter. Over the central U.S.A., the tropopause height usually varies between 30,000 ft (10 km) in winter and 50,000 ft (16 km) in summer and is close to the maximum height to which thunderstorms grow.

On stormy days, the temperature of the layer of drier air decreases more rapidly with height than normal so that rising air remains warmer than its environment, especially when there is abundant moisture and, correspondingly, a substantial contribution of heat from the condensation that occurs during ascent. Forecasters estimate the buoyancy of an airmass by lifting an imaginary parcel of air, assuming it cools as it rises at 5.5°F/1,000 ft (10°C km^{-1}) until saturated. They also assume the temperature at ground level reaches the maximum temperature forecast for the day. After saturation, at a level several thousand feet above ground, a slower saturation adiabatic lapse rate (3°F/1000 ft (5.5°C km^{-1}) is assumed. The difference between the imaginary parcel's temperature when lifted to 8,000 ft (6 km, 500 mb air pressure) and the actual temperature is called the LIFTED INDEX. Values of 0° to -10°F (0°C to -6°C) indicate conditions favorable for severe storm maintenance, and greater negative differences are cause for even more serious concern.

A significant feature that often precedes severe storms including tornadoes is a veering of wind direction with height (i.e., direction of air motion changes from south or southeasterly near the ground to southwesterly or westerly near the tropopause, with speed increasing with height. This direction and speed "shear" provides relative momentum and organizes the storm so that it can maintain itself over long periods of time.

A feature of the atmosphere's vertical structure which retards storm development until energies are released almost explosively, sometimes in less than 30 minutes, is a capping inversion at the top of the low-level moist layer (Fulks, 1949; Zittel, 1976). In an inversion layer, air temperature rises rather than falls with increasing height. Because of the inversion, the ground heats more than normally and all the moisture in the lower layers is held there until heating destroys the inversion and vertical mixing can proceed through a greater depth.

In the early spring, low-level stratus clouds are common and may somewhat reduce surface heating by the sun. On these severe storm days, strong air flow and relatively cold temperatures aloft can compensate for reduced surface heating.

Temperature inversions often are accompanied by a region of strong winds, the low-level jet. Sometimes, sustained winds of 60 kts (30 m sec^{-1}) or more are spotted as low as 1500 ft (.5 km) above ground, which strengthen transport of the low-level moisture required for severe storm initiation and maintenance.

Very often surface heating is not enough to start convective growth which leads to severe storms. Without convection (upward air currents induced by solar heating) other mechanisms may lift the low-level moisture high enough for condensation to begin, and the heat latent in the water vapor to become available to initiate and maintain thunderstorms. Fronts and subsynoptic low pressure areas are often effective in this way. These features, including surface heating, have one thing in common--they all produce localized convergence of low-level air.

Cold fronts lift moist air as they advance and thus initiate storm-scale convection. The actual preferred place for severe storms to form is about 50 miles (90 km) ahead of a cold front. Some low-level air, instead of being lifted over a cold front, moves parallel to it, becoming a clearly-defined boundary of warm moist air moving rapidly northward. Marked as a warm front, the leading edge intersects the developing squall line ahead of the cold front and increases the severity of storms near the intersection.

In the Great Plains (New Mexico, Texas, Oklahoma, Kansas, Nebraska and the Dakotas) a unique feature forms; a dry-line marks the westward extent of moisture from the Gulf of Mexico. Across this meteorological boundary, typical dewpoint temperatures vary from 60°F (15°C) or more on the eastern side, to 30°F (-1°C) or less on the dry western side. Diurnally, the dry-line boundary tends to move westward at night and eastward during the daytime (Schaefer, 1973). Winds generally are southwesterly or westerly on the western side and southeasterly on the eastern side. Hence, convergence takes place along this boundary. A favored time for storms to form along or near the dry line is mid-afternoon.

Often, a low pressure area forms along a front or dry line. This Low, with a diameter of some 100 miles (190 km) smaller than the Lows commonly seen on weather maps, is called a subsynoptic Low. Like the larger synoptic scale Low, this smaller scale feature quickens storm formation by providing upward vertical motion due to convergence (Tegtmeier, 1974).

To summarize this meteorology discussion, severe storms are more likely to form when special conditions are present: (1) strong southwesterly winds aloft with southerly or southeasterly winds at the earth's surface, (2) an upper layer of cold dry air, and (3) some mechanism to lift the moist surface air locally to the height where condensation forms. There, with the cloud-air warmer than the surrounding air, upward vertical growth continues in response to buoyancy.

Fawbush, Miller, and Starrett (1951) give a more rigorous treatment of the synoptic conditions leading to severe storm genesis. Moreover, they point out that the problem of forecasting severe storms is one of time and place, since favorable meteorological conditions are a coincidence of provocative factors.

Winds aloft strongly influence storm type. Strong winds aloft and substantial increase of wind with height associate with severe storms in rapid motion and with squall lines. When there is abundant moisture and strong surface heating but only light winds aloft, summer-type thunderstorms are likely. These are usually short-lived, existing only for an hour or so, and while these are heavy showers, the hazards they pose are principally to aircraft, and not to persons and property on the ground.

2.2 Climatology

2.2.1 Seasonal and diurnal variation

Severe storm occurrences adjust to the position of the jet stream, which fluctuates seasonally between a usual wintertime position over the Gulf Coast and a summertime one over southern Canada. Tornadoes are indicators of the geographic distribution of severe storms (Wolford, 1960). In January, February, and March, storms are relatively uncommon, but most likely in the Gulf states of Florida, Georgia, Alabama, Mississippi and Louisiana (Figure 1a). Oklahoma, Arkansas, Kansas, and Missouri mostly have tornadoes in April, May, and June. (Figure 1b). Thereafter in May, June, and July, tornadoes are likely northward into Iowa, Minnesota, Nebraska, and the Dakotas; June for this region is the month of highest frequency (Figure 1c). And a second peak in tornado frequency is found in Massachusetts in June.

The time of maximum occurrence of tornado-producing storms settles in the late afternoon between 1700 and 1800 LST in states not bordering the Gulf of Mexico (Figures 2a and 2b). But along the Gulf coast itself, maximum severe storm occurrence happens an hour earlier, and the daily maximum is not nearly as marked as further inland (Figure 2c).

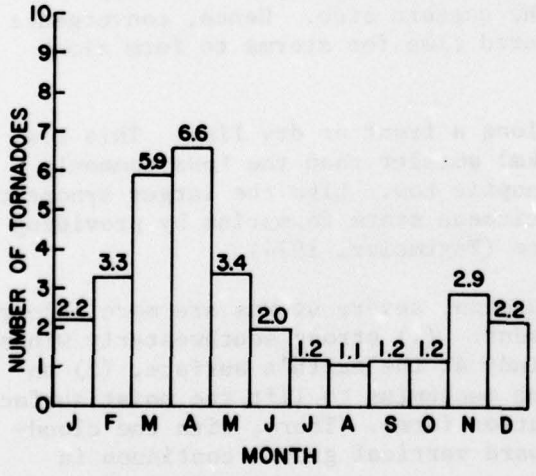

Figure 1a. Mean monthly number of tornadoes in the Alabama-Florida-Georgia-Louisiana-Mississippi area, 1916-58. (From Wolford, 1960.)

The time of maximum severe storm occurrence is not always the time of maximum thunderstorm occurrence. Brandes (1973) found that during one early Oklahoma spring the maximum number of storms occurred at 0300 LST, and Rasmusson (1971) found an early morning maximum of thunderstorm frequency at Oklahoma observing stations in summer. Brandes also found that at 1900 LST, when the number of storms was least, their size was largest. Many other climatological details await a more comprehensive data base.

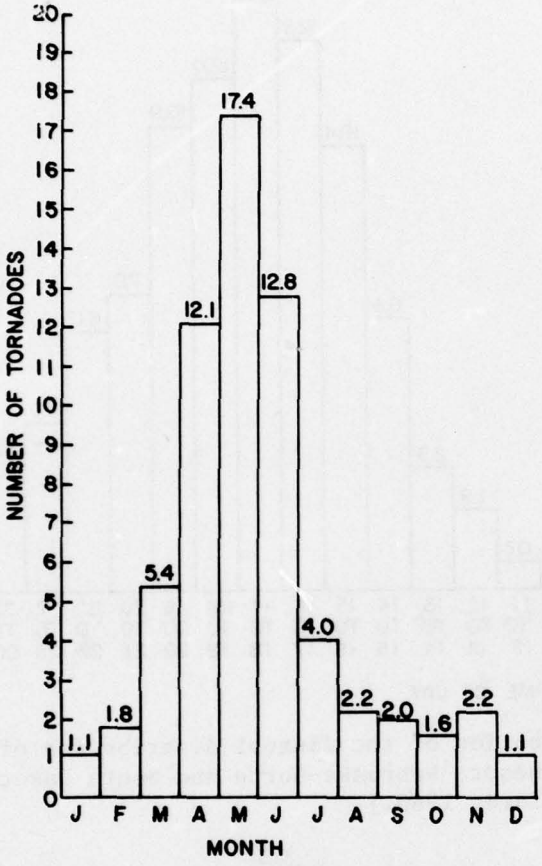

Figure 1b. Mean monthly number of tornadoes in the Arkansas-Kansas-Missouri-Oklahoma area. (From Wolford, 1960.)

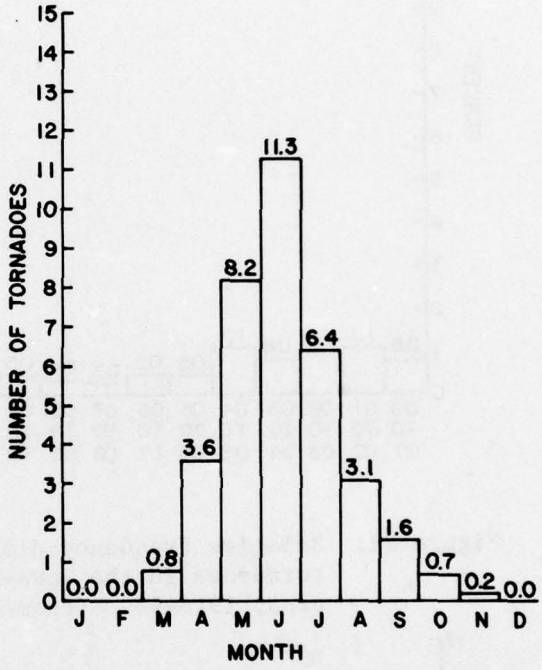

Figure 1c. Mean monthly number of tornadoes in the Iowa-Nebraska-North and South Dakota area. (From Wolford, 1960.)

2.2.2 Geographical considerations

The distribution of tornadic storms already has been indicated but is worth summarizing: Tornadic storms are most frequent over the central United States; tornadoes are rare and relatively weak west of the Rocky Mountains.

Hail 3/4 inch or larger in diameter is a hallmark of severe thunderstorms. A center of hail frequency occurs in northeastern Colorado and southeastern Wyoming during the summer months (U.S. Weather Bureau, 1947)(Figure 3). Note that a hailstorm, by definition, must deposit hail on the ground. Many thunderstorms do have hail aloft, but where the level of the 32°F (0°C) wet-bulb isotherm is high above the surface, the hail melts before reaching the ground. Lack of hail at the ground in warm climates does not guarantee lack of hail aloft!

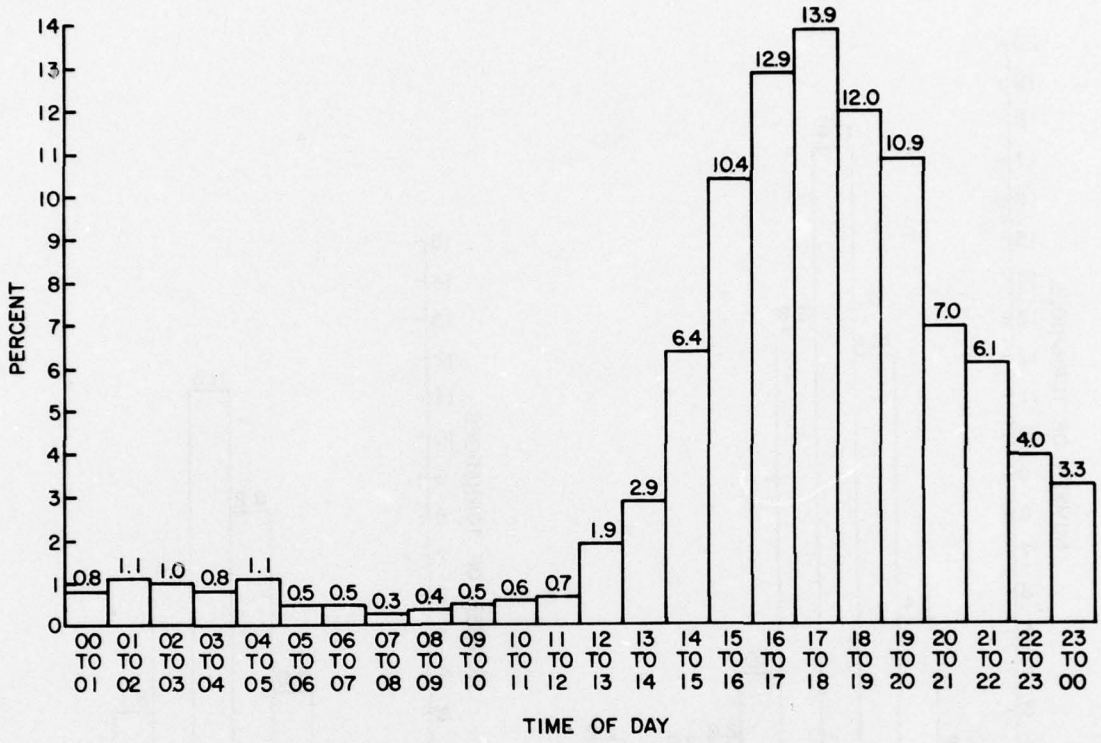

Figure 2a. Relative frequency distribution of the diurnal distribution of tornadoes in the Iowa-Minnesota-Nebraska-North and South Dakota area, 1916-58. (From Wolford, 1960.)

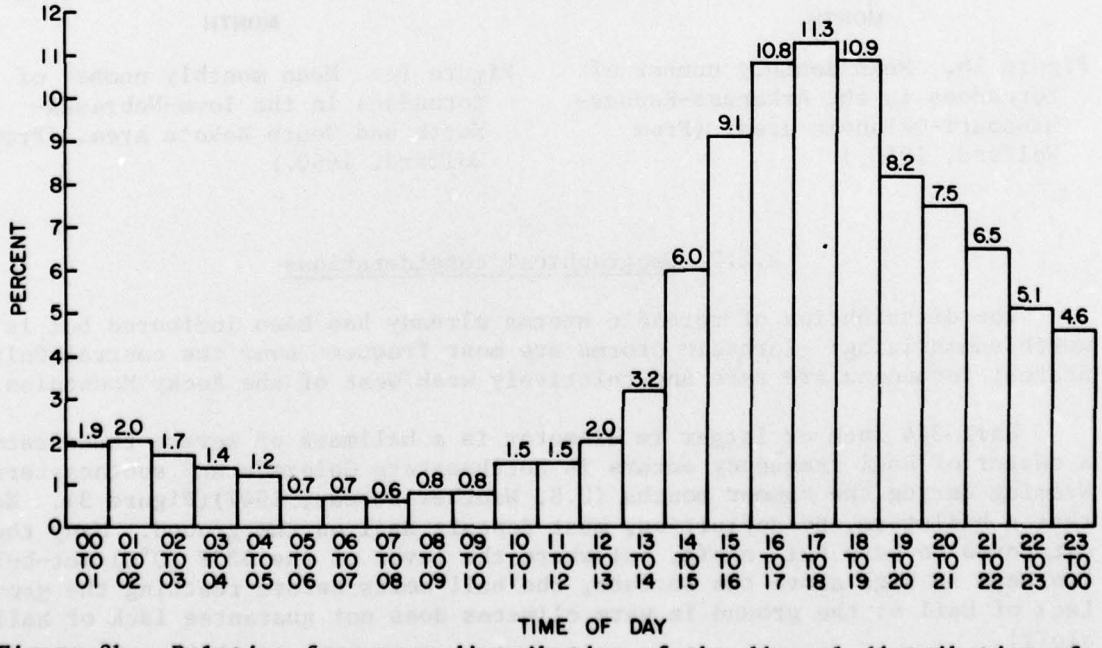

Figure 2b. Relative frequency distribution of the diurnal distribution of tornadoes in the Arkansas-Kansas-Missouri-Oklahoma area. (From Wolford, 1960.)

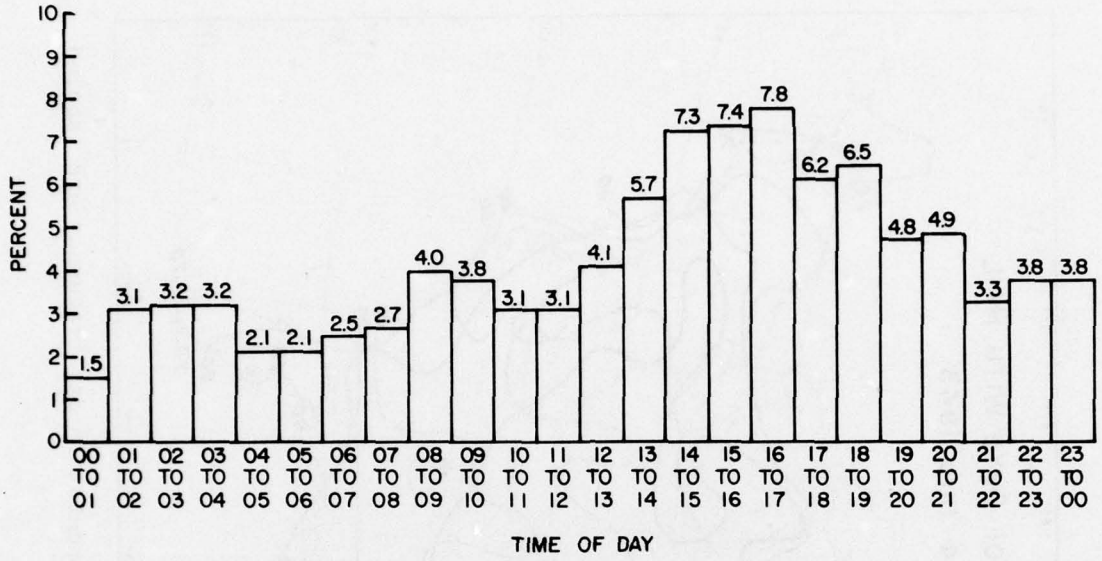

Figure 2c. Relative frequency distribution of the diurnal distribution of tornadoes in the Alabama-Florida-Georgia-Louisiana-Mississippi area. (From Wolford, 1960.)

A waterspout is a tornado-like whirlwind over a large body of water. A lesser whirlwind more akin to dust devils in size and strength also may be called a waterspout (Golden, 1974). The lesser vortex (common in southern Florida summers, especially the Keys region) forms under cumulus clouds over shallow, warm water. But any waterspout is hazardous and should be avoided.

Hurricanes, another class of severe storms along the Gulf Coast over water and land, sometimes produce severe thunderstorms and even tornadoes in their outer fringes. But because hurricanes form slowly and live long as compared to thunderstorms, they can be easily avoided by aircraft.

2.3 Storm Structure*

2.3.1 Severe thunderstorms

Several categories of thunderstorms such as squall lines, multiple cell, supercell, and severely sheared storms are identifiable (Marwitz, 1972a, 1972b, 1972c, and Chisolm, 1973). Non-severe multicell thunderstorms consist of a group of co-existing cells: each cell has an updraft-downdraft couplet. The typical life cycle, first documented by Byers and Braham (1949), from data collected during the Thunderstorm Project, is characterized by three stages. In the cumulus stage, only updrafts exist with no rainfall. In maturity, both updrafts and downdrafts occur with the rainfall rate at a maximum. During the dissipating stage, downdrafts prevail and rainfall is light.

*Much is drawn from NWS Tech. Memo. NWS NSSFC-1 by L. R. Lemon.

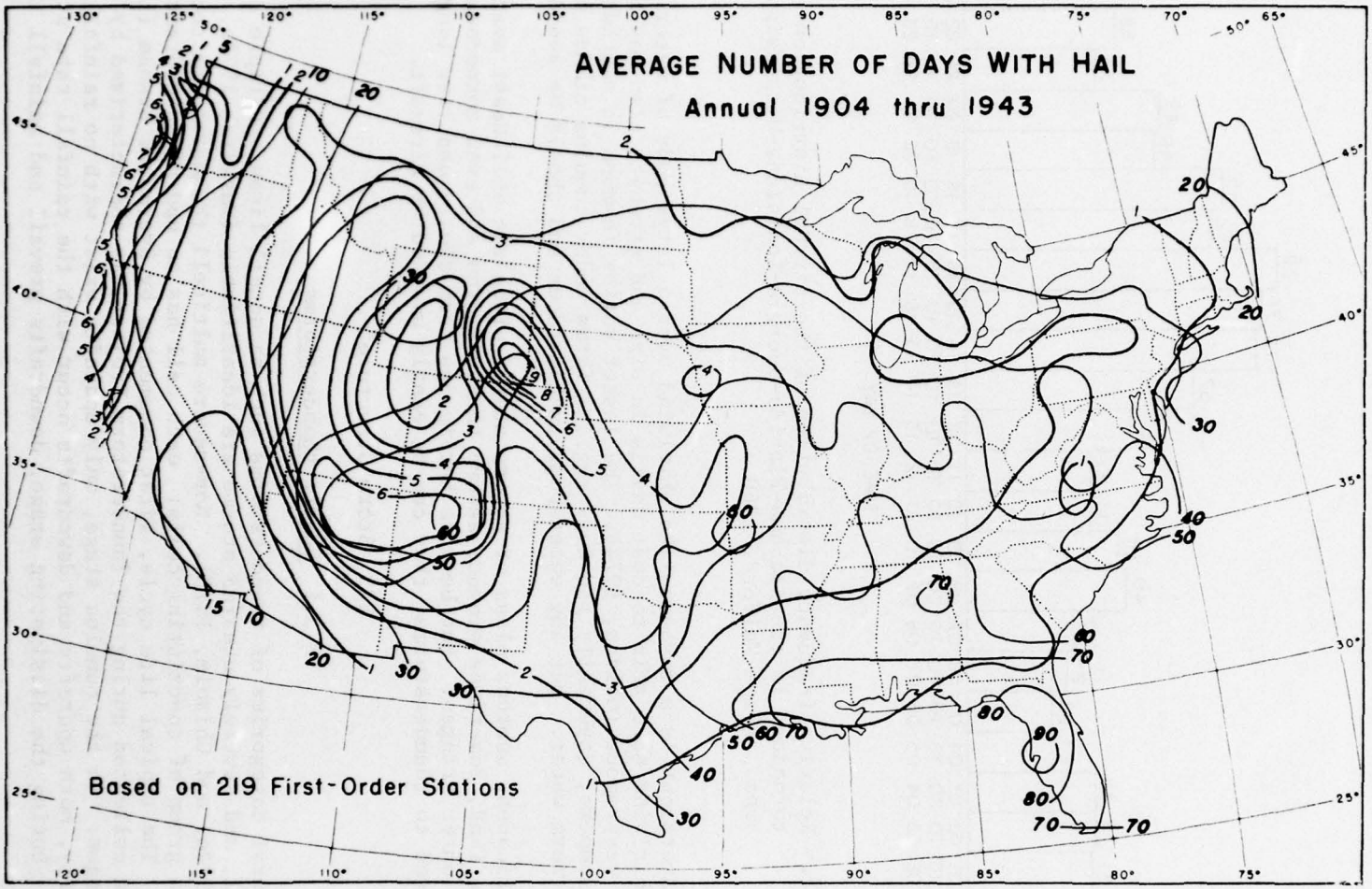

Figure 3. Average number of hail days. Lines of equal thunderstorm day frequency are labeled in bold type. (From U.S. Weather Bureau, 1947.)

A small but significant number of thunderstorms substantially produce only one large persistent cell which usually travels to the right of and slower than the atmosphere's mid-level steering winds. Such "supercells" retain only one co-existing updraft and downdraft. The structure, which lasts many times longer than the time air takes to pass through the storm, is in a quasi-steady state.

The earliest thunderstorm development goes undetected by most radars because there are no precipitation-size hydrometers (rain, snow, etc.) to be seen; only a large cumulus cloud or collection of cumulus clouds in rapid growth is visible. Because of very cold temperatures (-40°F or C), when a growing cumulus cloud reaches upper levels condensation is in the form of ice crystals; these stream downwind of the storm to make the familiar anvil top of a cumulonimbus cloud.

Precipitation-sized particles usually first form between 15,000 and 30,000 ft (5 and 10 km). With stronger updrafts, first precipitation forms at greater heights and often signifies a more severe storm (Browning and Atlas, 1965; Burgess and Lemon, 1976). Drops grow within the updraft by condensation and by collecting small drops in their paths. Water-loading and cooling by evaporation into entrained ambient air weaken the updraft and may finally turn the updraft into a downdraft. The shower cycle is most common in no-shear conditions, but the showers may be very tall and produce locally heavy rainfall and gust fronts with strong winds.

When wind shear conditions favorable for severe storms are present, the updraft tilts downstream and the rain tends to be removed horizontally from the updraft, to fall into an adjacent downdraft (Figure 4a). Figure 4b, a plan view of the storm in an early non-violent stage, shows the distribution

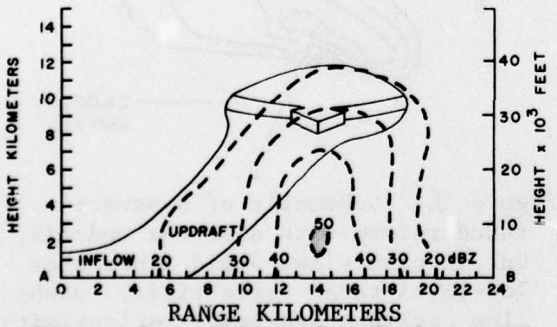

Figure 4a. Schematic of the vertical cross-section of a moderate thunderstorm radar reflectivity (dashed lines) in a sheared environment. Areas >50 dBZ are stippled; solid lines show inflow from left to right, a moderate updraft, and outflow aloft directed outward.

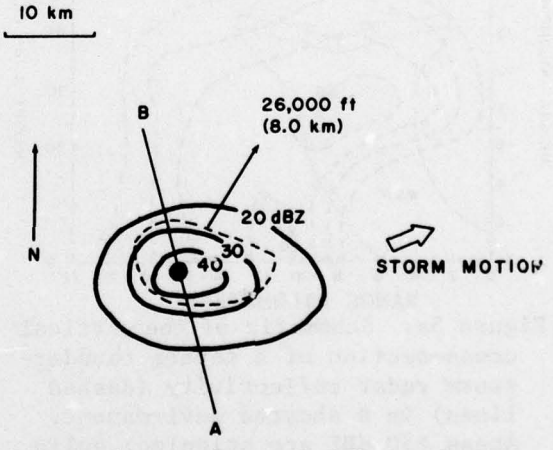

Figure 4b. Schematic of a moderate thunderstorm, but in plan view. Solid lines show low-level radar reflectivity. Dashed line outlines mid-level reflectivity ≥20 dBZ. Black dot shows position of highest echo top. Line AB is the cross-sectional axis of 4a.

of hydrometers (rain, hail, etc.) near the ground. Also note the 20 dBZ* contour of the mid-level echo and a black dot indicating the storm top.

The transition from moderate to severe requires that the updraft be stronger. When the updraft is more vigouous, the winds in the storm environment have less influence and the stronger updraft assumes a more erect position (Figure 5a). Maintenance of a stronger updraft requires stronger convergence of the low-level moist air. Convergence may result from a synoptic or subsynoptic low pressure system or from unique configurations of other storms nearby which channel the moist air into a favored area.

A stronger and more nearly vertical updraft can produce hail and large raindrops which, because of their mass, are not blown far from the updraft by mid-level winds. When these particles fall out, they produce sharp changes in rainfall rates over short distances. These changes correspond to strong reflectivity gradients on the right rear storm flank (Figure 5b). Generally, the highest rainfall rate associates with the highest reflectivity and is adjacent to the updraft in severe storms. The storm top usually is found over the reflectivity gradient.

As moist air converges faster and over a longer time, the updraft (visible as a tower) becomes more intense and begins to rotate. The strong updraft forces the strongly sheared environmental flow to diverge around it and is marked by an area of weak echo, the bounded weak echo region (Figure 6a).

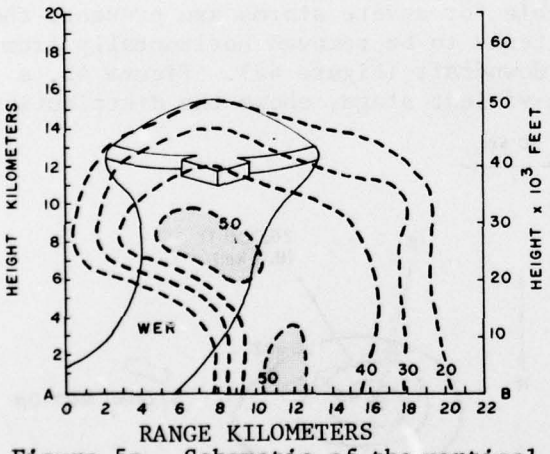

Figure 5a. Schematic of the vertical cross-section of a severe thunderstorm radar reflectivity (dashed lines) in a sheared environment. Areas >50 dBZ are stippled; solid lines show inflow from left to right, a strong updraft, and outflow aloft directed outward.

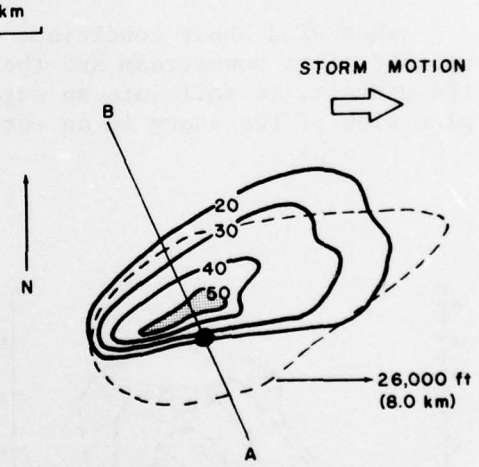

Figure 5b. Schematic of a severe thunderstorm with a strong updraft, but in plan view. Solid lines show low-level radar reflectivity. Dashed line outlines mid-level reflectivity ≥20 dBZ. Black dot shows position of highest echo top. Line AB corresponds to cross-sectional axis of 5a.

*Reflectivity of precipitation is proportional to the amount of radar energy reflected by the precipitation. In practice, a quantity Z, the reflectivity factor is commonly used; this is proportional to reflectivity itself and is expressed in decibels dBZ, referred to Z=1. (See Appendix A)

As rotation strengthens, a mesocyclone forms at mid-levels in the southwest (right rear) quadrant of the storm. A large downdraft area coincides with the heaviest precipitation and usually forms north and east of the mesocyclone. Mid-level dry air mixes with the precipitation; the air cools by evaporation of some of the precipitation, becomes colder than the surrounding air, and sinks.

As a mesocyclone intensifies, precipitation is drawn inward by the circulation and rain and hail reach the ground southwest of the mesocyclone. Evaporatively cooled air descends and forms a localized cold front boundary or gust front between itself and the warmer inflow air, very similar to synoptic frontal patterns (Brandes, 1977). Later, the precipitation echo behind the cold gust front sometimes assumes the hook or pendant shape shown in Figure 6b. Gust front structure is complicated and is explained further in section 2.3.2 on squall lines.

Cyclonic shear may be enhanced by the cold air outflow, and thereby intensify the mesocyclone near the surface. This intensification makes tornado formation more likely. At times, however, the cold air outflow can cut off the updraft's moisture supply; then the mesocyclone fills and precipitation, which was suspended aloft, falls. Sometimes, as one mesocyclone updraft

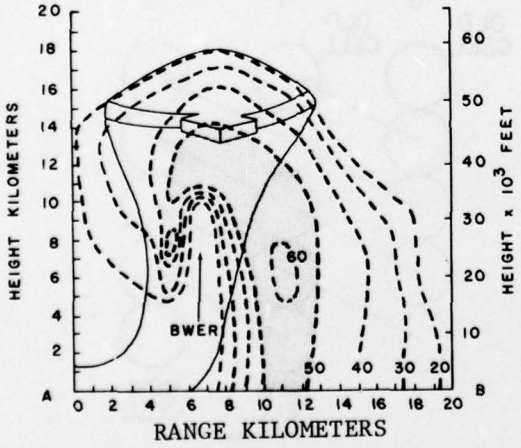

Figure 6a. Schematic of the vertical cross-section of a severe thunderstorm radar reflectivity (dashed lines) in a sheared environment. Areas >50 dBZ are stippled; solid lines show inflow from left to right, an intense updraft, and outflow aloft directed outward.

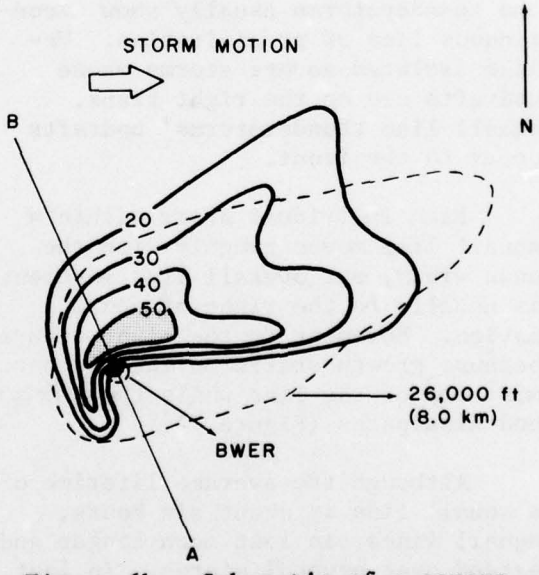

Figure 6b. Schematic of a severe thunderstorm with an intense updraft, but in plan view. Solid lines show low-level radar reflectivity. Dashed line outlines mid-level reflectivity ≥20 dBZ. Black dot shows position of highest echo top. Line AB corresponds to the cross-sectional axis of 6a.

region is weakening, a new one, forward (eastward) of the old position forms, intensifies, and thus sustains the severe storm state. Darkow (1971) reported storms which produce tornadoes repetitively at intervals of about an hour.

A key to supercell maintenance is availability of low-level warmth and moisture from which to feed a mesocyclone. If the moisture is cut off, the storm weakens or dissipates.

Although supercell storms are a small fraction of all thunderstorms, they cause a disproportionate amount of damage. In a two-year study of 17 multicell and 10 supercell hailstorms in Oklahoma, Nelson (1976) found that the average maximum hail size for multicell storms is 3/4 inch (2 cm), but the average for supercells is 2 inches (5 cm). The average maximum hail swaths are 5.8 n mi (10.7 km) for multicells and 10.9 n mi (20 km) for supercells. Eight of ten supercells generated severe weather other than hail. Only four of the multicell storms produced severe weather; none produced tornadoes. Severe storms often travel rapidly, even 60 kts (30 m sec^{-1}) or more, though this is not so fast as the strongest winds aloft.

2.3.2 Squall lines and gust fronts

Squall lines are narrow bands of active thunderstorms. On a radar PPI, the thunderstorms usually show a continuous line of precipitation. Unlike isolated severe storms whose updrafts are on the right flank, squall line thunderstorms' updrafts occur to the front.

Each individual storm within a squall line moves roughly with the mean winds, but overall line movement is usually to the right of storm motion. Movement to the right occurs because growth starts on the southernmost end of the line while the northern end dissipates (Figure 7).

Although the average lifetime of a squall line is about six hours, squall lines can last much longer and extend over several states. In fact, squall lines commonly enter western Oklahoma from the Texas panhandle in late afternoon of one day, then by early morning of the next day are entering Arkansas.

Cold outflow air from the many individual storms in a squall line

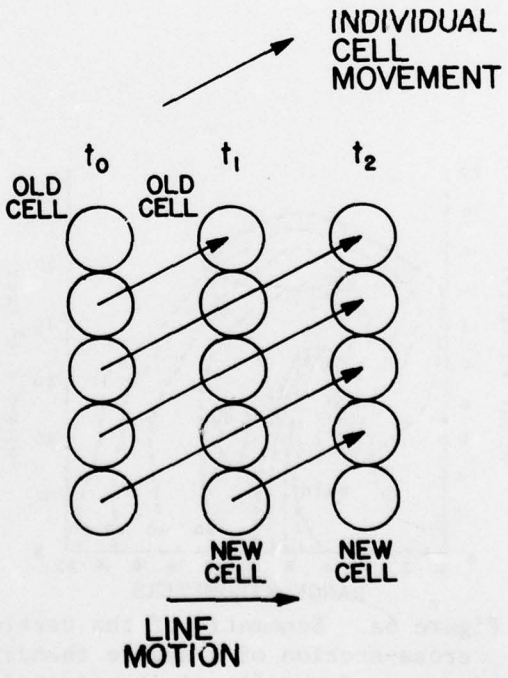

Figure 7. Schematic of squall line comparing individual cell (storm) motion to line motion. Old cells dissipate at the northern end while new cells form at the southern end.

combines to produce a gust front parallel to the line of storms. This gust front has many properties of the larger scale cold front, as shown in Figures 8a and 8b. Gust fronts are characterized at the surface by a change in wind direction (usually veers clockwise from a southerly to a westerly direction) and one or more of: (1) a sudden rise in pressure, (2) a sudden increase in wind speed and gustiness, and (3) a sudden drop in temperature concurrent with another rise in pressure. Goff (1975) identified four gust front types. They are: (a) gust fronts associated with intensifying storms or accelerating outflow; (b) gust fronts with mature, intense storms or strong outflow; (c) gust fronts with dissipating storms or outflow decelerating as related to the parent storm; and (d) gust fronts in the final stage of life cycle. Roughly, types a and b correspond to the Byers and Braham mature stage and types c and d to the dissipating stage. A wide time and space separation between a gust front and the onset of rain occurs in many mature storms, but gust fronts do not always precede the onset of rain. Average forward speed of the 20 cases Goff studied was 20 kts (10 m sec^{-1}), but maximum windspeeds within the gust front can reach 60 kts (30 m sec^{-1}) or stronger. The gust front often has the strongest, most turbulent winds of the entire storm.

The gust front structure (Figure 8c) often shows a protruding nose and a substantial head of piled-up air because surface features retard air flow near the ground. Highest speeds occur midway through the depth of cold air outflow. To an observer moving with the gust front a backflow appears near the ground, but to a stationary observer the wind continues to blow away from the storm. The upward tilt of the gust front's leading edge seems more nearly vertical with outflow from mature storms than from intensifying and dissipating storms.

Air ahead of a gust front is lifted upward in a thin band, usually between one-half and one mile (1 to 2 km) in width. In intense gust front situations, vertical motions may exceed 20 kts (10 m sec^{-1}); some gust fronts reach a depth of 3000 ft or 1 km (Bedard and Beran, 1977). Gust

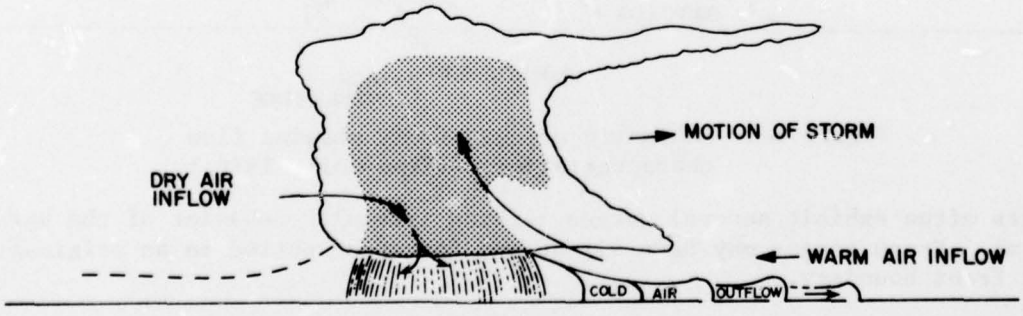

Figure 8a. Schematic of the vertical cross-section of a squall line along the direction of motion. Stippling shows areas of rain and suspended precipitation aloft. Multiple surges in the gust front are shown. (From Goff, 1976.)

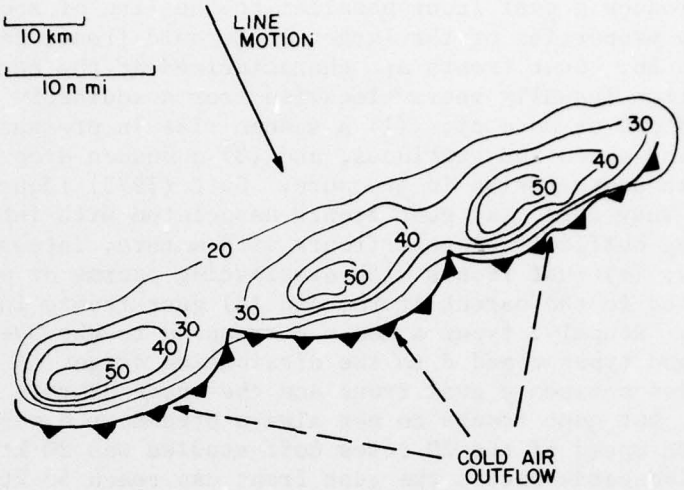

Figure 8b. Schematic of a squall line in plan view. Cold air outflow shown as barbed line.

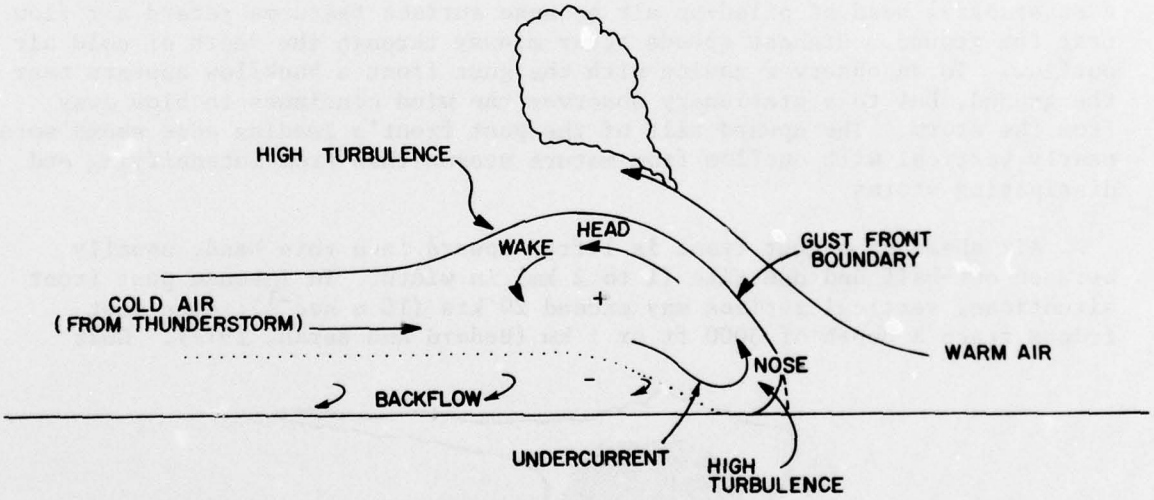

Figure 8c. Schematic of gust front showing flow characteristics. (From Goff, 1976.)

fronts often exhibit several surges marking irregular behavior of the parent storms. Fresh surges may have all or any features spotted in an original gust front boundary.

Goff explains that within gust fronts, turbulence is high in the nose and also in the wake of the head. Of course, one of the severest hazards to aircraft landings and take-offs is the marked change in lift and ground speed that accompanies flight through changes in wind speed and direction along a gust front's leading edge. A study using flight simulators shows that during landings and take-offs, pilots are probably unable to compensate

adequately for marked changes of wind that accompany thunderstorms (Conelly, 1977).

2.4 Information Sources to Forecast, Detect, and Report Severe Storms

In 1952, the U.S. Weather Bureau established the Severe Local Storms Unit (SELS) to forecast severe thunderstorms and tornadoes routinely. Started in Washington, D. C., the unit was moved to Kansas City in 1954. In 1966, the National Severe Storms Forecast Center (NSSFC) was formed with SELS (Mogil and Groper, 1977).

Procedures and policies to spread forecasts and warnings, begun in 1967, at the request of the Federal Coordinator for Meteorological Services and Supporting Research, are outlined each year in a National Severe Local Storms Operation Plan (Epstein, 1977). Aviation severe weather forecasts flow through the Flight Advisory (FA) Centers to Flight Service Stations (FSS) and Air Route Traffic Control Centers via FAA Service A (Figure 9). In

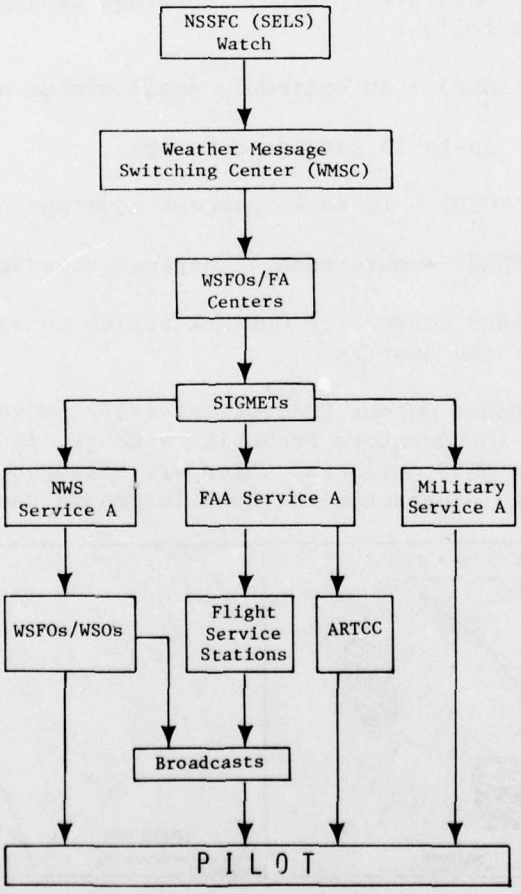

Figure 9. Schematic of distribution of aviation severe weather forecasts. (Adapted from Epstein, 1977.)

addition, there are local arrangements whereby Terminal Radar Control Centers (TRACONS) receive bulletins, pertinent hourly sequences and special observations via TelAutographic writers from FSS and NWS offices.

On the basis of surface and upper air data, the National Meteorological Center (NMC) prepares forecast charts as much as three days ahead. These forecasts facilitate outlooks on major tornado and severe storm outbreaks that are foreshadowed by NSSFC a day and a half in advance. In severe storm situations, advance notice passes to each National Weather Service Forecast Office (NWSFO) in the affected area.

Severe weather outlooks are issued routinely by the SELS forecaster at 0830 and 1500 Greenwich Mean Time (GMT) and are valid for a period through 1200 GMT of the following day. In addition, between February 1 and August 31, a 1900 GMT outlook is issued. Severe weather outlooks are available on the RAREP (radar report) and Warning Coordination (RAWARC) teletype circuit. Also, the 0830 GMT outlook is available graphically on the National and Aviation Meteorological Facsimile Circuit (NAMFAX) at 1000 GMT (Figure 10). As needed, the SELS outlooks are updated. Coverage designations for the expected severe thunderstorms follow:

A. Isolated (ISOLD) - an extremely small number are expected.

B. Few (FEW) - up to 15 percent coverage.

C. Scattered (SCTD) - 16 to 45 percent coverage

D. Numerous (NMRS) - more than 45 percent coverage.

The area in a SELS Convective Outlook varies considerably from a single state to sections of the country.

At 1300 GMT a Model Output Statistical (MOS) prognostic chart, the Thunderstorm/Severe Thunderstorm Probability Chart, is issued on NAMFAX (Figure 11). Unlike SELS outlooks, which are based on atmospheric dynamics and the forecaster's interpretation, such forecasts use climatologically

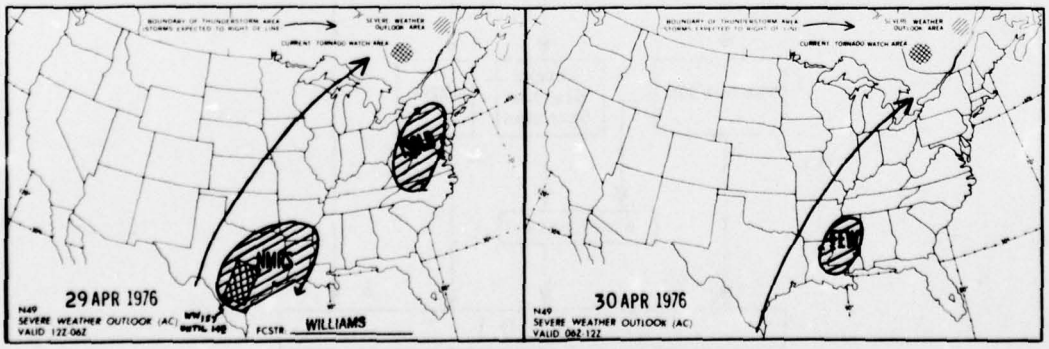

Figure 10. Sample convective (severe weather) outlook graphic. (From Mogil, 1977.)

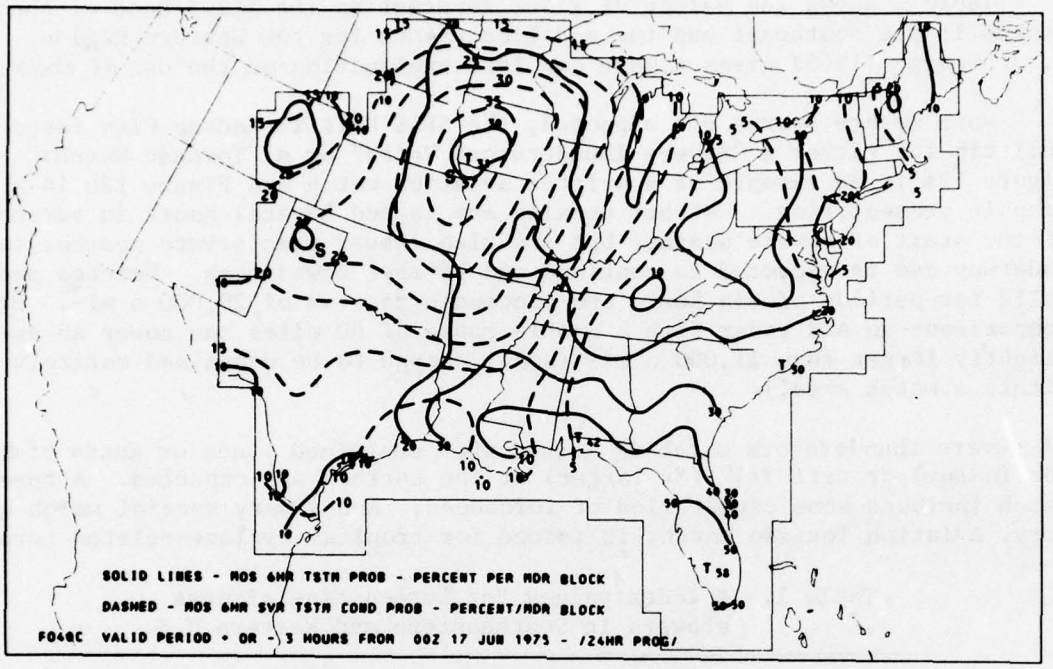

Figure 11. Sample thunderstorm/severe thunderstorm probability prognostic chart. (From Mogil, 1977.)

derived predictors which "...have a dual role, namely to simulate seasonal variations in thunderstorm and severe local storm occurrence and to modulate the climatology by the daily synoptic situation" (Reap, 1977).

On the REQUEST/REPLY teletype circuit, linked to the FAA computer in Kansas City, Missouri, is a Two-to-Six Hour Probability of Thunderstorms and Severe Weather Forecast product. Radar and surface data at 1500, 1800, 2100, and 0000 GMT are used in conjunction with predictors to provide forecasts two to six hours in advance. These forecasts usually are available one hour after the surface and radar observations (Charba, 1977).

About 1630 GMT, a composite moisture chart is available on NAMFAX. The composite contains a Lifted Index/K Index Chart, a Precipitable Water Chart, a Freezing Level Chart, and an Average Relative Humidity Chart. The first chart presents estimated storm probabilities. Both the Lifted Index and the K Index combine temperature and moisture parameters into a single value; but whereas the Lifted Index (see sec. 2.1) is suited for forecasting the likelihood of severe storms, the K Index is better suited for summer or airmass thundershowers (i.e., conditions of weak winds aloft). The K Index, developed by R. M. Whiting for forecasting airmass thunderstorms over the southeastern United States, applies also to forecasting thunderstorms over the western United States (Hambidge, 1967). The formula for computing K is:

$$K = (850\text{ mb temp} - 500\text{ mb temp}) + (850\text{ mb dewpoint}) - (700\text{ mb dewpoint depression})$$

Table 1 shows the values of K for forecasting the likelihood of thunderstorms in the Southeast and the modified values for the Western Region. J. J. George (1960) gives a more complete explanation on the use of the K Index.

When severe storms are expected, the SELS Unit in Kansas City issues a bulletin for either a "Severe Thunderstorm Watch" or a "Tornado Watch." Figure 12a is an example of a written aviation watch and Figure 12b is a graphic presentation. Watches usually are issued several hours in advance of the start of severe weather but are also issued when severe weather is underway and is expected to continue and to move downstream. Watches are valid for periods of six hours and encompass an area of 20,000 n mi^2. By comparison--an ASR radar with a usable range of 60 miles can cover an area slightly larger than 11,000 n mi^2 (small enough to be contained entirely within a watch area!).

A severe thunderstorm watch is issued when sustained winds or gusts of 50 kts (or faster) or hail 3/4" (or larger) at the surface are expected. A tornado watch includes some expectation of tornadoes. And a very special watch category, Aviation Tornado Watch, is issued for tropical cyclone-related tornadoes.

Table 1. K Index values for forecasting airmass showers in Southeastern and Western U.S.

Southeastern U.S.		
	K Value	Frequency Category
1.	Less than 20	None
2.	20 to 25	Isolated thunderstorms
3.	25 to 30	Widely scattered thunderstorms
4.	30 to 35	Scattered thunderstorms
5.	Greater than 35	Numerous thunderstorms

Western U.S. (Western Plains to Pacific Coast)		
1.	Less than 15	0%
2.	15 to 20	Less than 20%
3.	20 to 25	20 - 40%
4.	25 to 30	40 - 60%
5.	30 to 35	60 - 80%
6.	35 to 40	Greater than 80%
7.	40 to 45	Near 100%

BULLETIN
AVIATION TORNADO WATCH NUMBER 290A
NATIONAL WEATHER SERVICE KANSAS CITY MO
1130Z FRI AUG 17 1972

20 STATUTE MILES S

A...ALG AND 90 STATUTE MILES EITHER SIDE OF A LN FM 90 STATUTE MILES NNE ORL TO //
DHN. THIS INCLS MOST OF NWRN FL...AND PTNS SERN AL AND SRN GA...VALID 171200Z-171800Z.

B...CONT WW 288A UNTIL EXPIRATION AT 12Z.

C...TORNADOES AND FEW SVR TSTMS...WITH HAIL ALF TO 1 1/2 IN...EXTRM TURBC AND SFC
WND GUSTS EXCEEDING 65 KT...A FEW CBS WITH MAX TOPS TO 500. MEAN WIND VECTOR 20040.

D...TORNADOES AND SVR TSTMS ASSOCD WITH HURCN AGNES.

MAGOR

Figure 12a. Sample Verbal Aviation Severe Thunderstorm Watch (From Epstein, 1977.)

A "Warning" issued by local WSFO's and WSO's may apply to severe thunderstorms, tornadoes, or both. Warnings are issued on a county-by-county basis and are valid for about an hour. The events for which warnings may be issued are the same as for watches but are based on radar data and public visual sighting reports. Both watches and warnings are transmitted over the RAWARC teletype circuit.

FA Centers (WSFO's with aviation responsibilities) issue Significant Meteorological Information Bulletins (SIGMETS) whenever severe weather is forecast or occurring. The expected events that trigger issuance of severe storm related SIGMETS are:

A. Tornadoes
B. Lines of thunderstorms or squall lines
C. Embedded thunderstorms
D. Hail 3/4" or larger in diameter
E. Severe or extreme turbulence
F. Severe icing

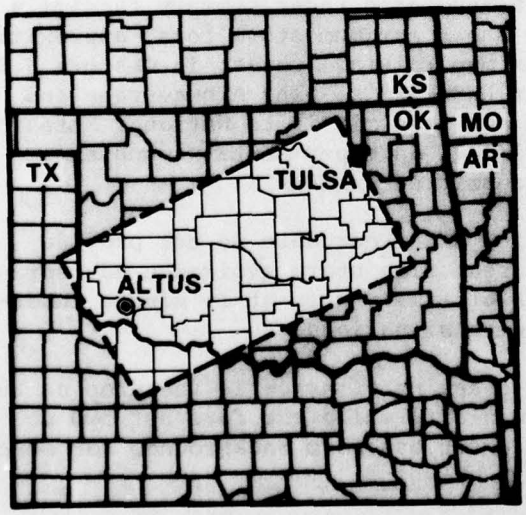

Figure 12b. Sample graphic of Severe Thunderstorm Watch. (From Mogil, 1977.)

It should be noted that the location of items B, C, and possibly D can be determined from present-day operational radar, but that A cannot; E and F are always present in severe storms but are not suited to detection by today's operational radar.

Under present FAA Instrument Flight Rules (Reg. 91.125, radio communications, sec. B) Pilots Reports (PIREPS) are required of pilots flying IFR whenever they encounter unforecast weather

conditions. And pilots ought to report every weather condition hazardous to aviation. The ARTCC's are requested to pass along these PIREPS to FSS's which are required to enter them on the Service A teletype circuit.

Additional information, in hourly radar reports (RAREPS) from NWS WSR-57's, is available on the RAWARC teletype circuit. These brief summaries give maximum rainfall rates for storms as deduced from radar, maximum storm tops, individual cell location and movement, and overall line movement when applicable.

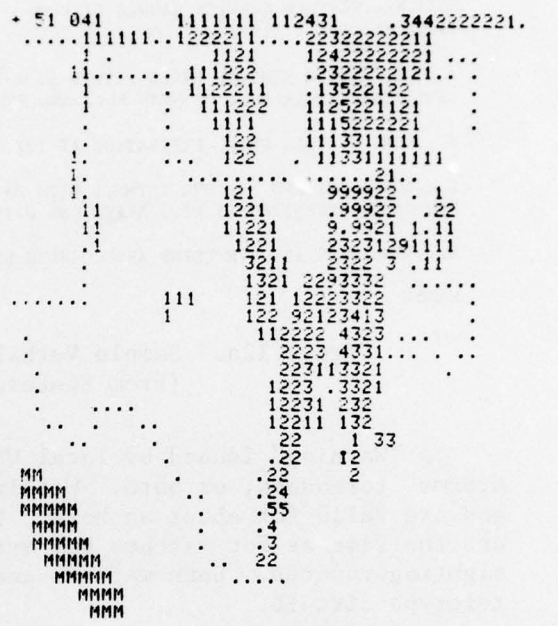

Figure 13. Sample REQUEST/REPLY teletype Radar Intensity Plot. M indicates radar out for maintenance.

Available from the REQUEST/REPLY teletype is a Manually Digitized Radar (MDR) Intensity Plot (Figure 13). Radar data are coded by rainfall intensity with different scales used for stratiform and convective systems. Rainfall rates relate to the digital numbers as shown in Table 2. Each number represents a 22 x 22 n mi area; the U.S.A. and borders are divided into six regions. This chart for each hour is ready about 30 minutes after the time of transmission of the radar observation from an NWS field site.

Also issued every 90 minutes is an annotated radar summary facsimile chart of the U.S.A. This U.S.A. chart shows maximum storm tops, approximate area of coverage, storm motion, and maximum rainfall rates; in western U.S.A., ARTCC radars provide radar coverage for NWS WSFO's. The Albuquerque and Salt Lake City WSFO's combine all data and transmit it to National Meteorological Center (NMC) in Suitland, Maryland. An experimental computer-generated Radar Summary Plot is now transmitted on NAMFAX.

It is an important fact that routine NWS radar data do not provide enough continuity in time or space for real time storm avoidance advisories to aircraft. For this purpose, updates of timely data at 15 minute intervals or less are required in fast-changing situations.

Other facsimile charts facilitate tracking of synoptic features as they develop. The 500 mb chart defines flow aloft, while the forecast 500 mb chart and the forecast vertical motion chart can form backgrounds for severe storm forecasts.

Photographs from the geostationary satellites are available every 15 to 30 minutes. Pictures from space offer supplemental synoptic information on cloud and thunderstorm complexes (Figure 14). However, the satellite photos

Table 2. Teletype Plot Numbers, Echo Intensities, Rainfall Rate Chart†

Teletype Plot Number	Echo Intensity	Rainfall Rate (in./hr.) Stratiform*	Convective **
1	Light	Less than 0.1	Less than 0.2
2	Moderage	0.1 - 0.5	0.2 - 1.1
3	Heavy	0.5 - 1.0	1.1 - 2.2
4	Very Heavy	1.0 - 2.0	2.2 - 4.5
5	Intense	2.0 - 5.0	4.5 - 7.1
6	Extreme	More than 5.0	More than 7.1
8-9	Unknown		

*Based on $Z = 200\ R^{1.6}$

**Based on $Z = 55\ R^{1.6}$, except 7.1, the threshold for extreme intensity, is empirically derived.

†For radar ranges greater than 70 nautical miles, one should use care in interpreting this table. That is, rainfall rates greater than those shown are possible.

Figure 14. Satellite picture of large thunderstorm complex over eastern Oklahoma, June 13, 1975. Other thunderstorms are located in the Texas Panhandle. (From Wilk et al., 1976.)

and almost all other data received via NAMFAX and RAWARC involve some lapse time and the data user must be alert to the fact that weather changes continually.

Twice daily the Central Flow Control Facility (CFCF) in Washington, D.C., briefs ARTCCs via conference calls concerning pertinent weather derived from all sources. When special observations are made, they are relayed to specific ARTCCs. But note that the majority of approach control radar facilities are NOT briefed by the CFCF.

Clearly, there is a plethora of storm data available from the NWS to assist the controller in making decisions about current weather. ASR radars, as is demonstrated in the next section, in their present operational modes do not provide enough information to be used as primary data sources about severe storms (as the WSR-57s are used). The proper role of the ASR radar is to supplement existing NWS products by providing the immediacy these products lack.

3. SCOPE INTERPRETATION OF SEVERE STORM ECHO PATTERNS FOR ASR SYSTEMS, GUIDELINES

Donaldson expressed the problem of identifying severe thunderstorms by radar when he wrote, "The identification of a severe thunderstorm by radar... depends on the observation of storm features which reflect either the intensity or persistent state of organization of the convective process" (1965). These complex features can be understood further in quantitative and qualitative terms. In this report only the qualitative aspects are applied to ASR radars. A survey of severe storm aspects that are correlated to intensity is included in Appendix B.

Qualitative characteristics cover three broad areas: (a) individual echo configuration; (b) distribution of echoes in relation to each other; and (c) echo motion. We are concerned with both isolated severe storms and with squall lines.

When using radar to identify severe storms, the character of each individual radar is as important as a storm's own features. Thus, the basic ASR operating modes as they affect weather presentations are considered.

3.1 ASR Parameters and Echo Interpretation

The FAA radars have many selectable and adjustable features including Sensitivity Timing Control, Moving Target Indicator, Receiver IF Response, Antenna Polarization, Low/High Beam (ASR-8) and Video Gain Setting. These are often adjusted to enhance aircraft detection. Some features are preselected on a site-by-site basis; others are adjusted or chosen on an as-needed basis by the controller to reduce ground and precipitation clutter.

On the other hand, weather surveillance radars can be set in fixed operational modes to make quantitative measurements. Therefore, with weather surveillance radars, changes in the scope display are usually interpreted in terms of weather changes.

3.1.1 Beam shape

Because of the need to monitor aircraft at various altitudes, FAA ASR radars are fan-shaped for the first 5°, and at higher elevation angles have a Csc^2 response. Generally, each facility selects a different vertical orientation because at each local site exposure conditions vary. Because of its beam shape, the ASRs average the return power from all precipitation within a pulse-volume of the atmosphere having a high vertical extent. Consider the severe storm (Figure 6) in section 2.3.1. If, to the low- and mid-level PPI echo contours (Figures 15a and b), we add the precipitation echo at upper levels (Figure 15c), we obtain the echo outline shown in Figure 15d.

A 34,000 ft storm will just fill a beam of 5° at 60 n mi (Figure 16). Therefore, at ranges less than 60 n mi some portion of the Csc^2 shape intercepts this storm. Offi indicates that this Csc^2 portion contributes negligible power for an ASR-7 radar when the storm at the given ranges also fills the 5° vertical fan beam (1977). The amount of return echo from an anvil which lies downstream of the heavy rain is limited by the combined effects of lower reflectivity, reduced antenna gain and partial beam filling.

3.1.2 Sensitivity time control

Sensitivity Time Control (STC) or range normalization is used to prevent saturation by ground clutter targets of the radar receiver and Moving Target Indicator (MTI) circuits, according to the FAA Primary/Secondary Terminal

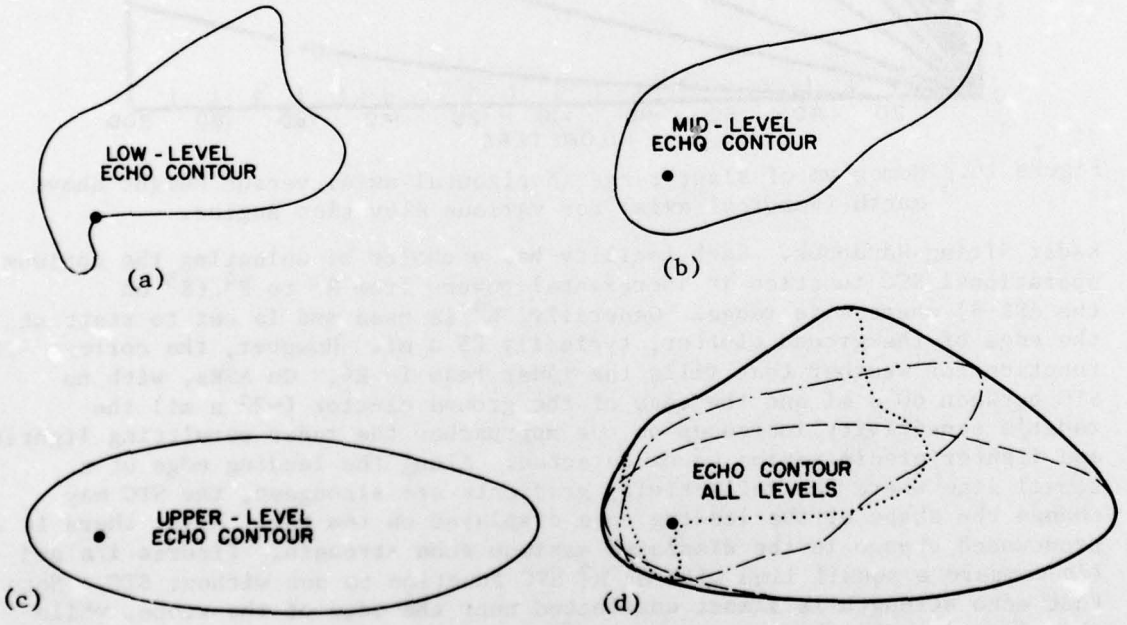

Figure 15. Schemati of severe thunderstorm in plan position showing (a) low-level, (b) mid-level, (c) upper-level, and (d) combined radar echo outlines due to vertical integration.

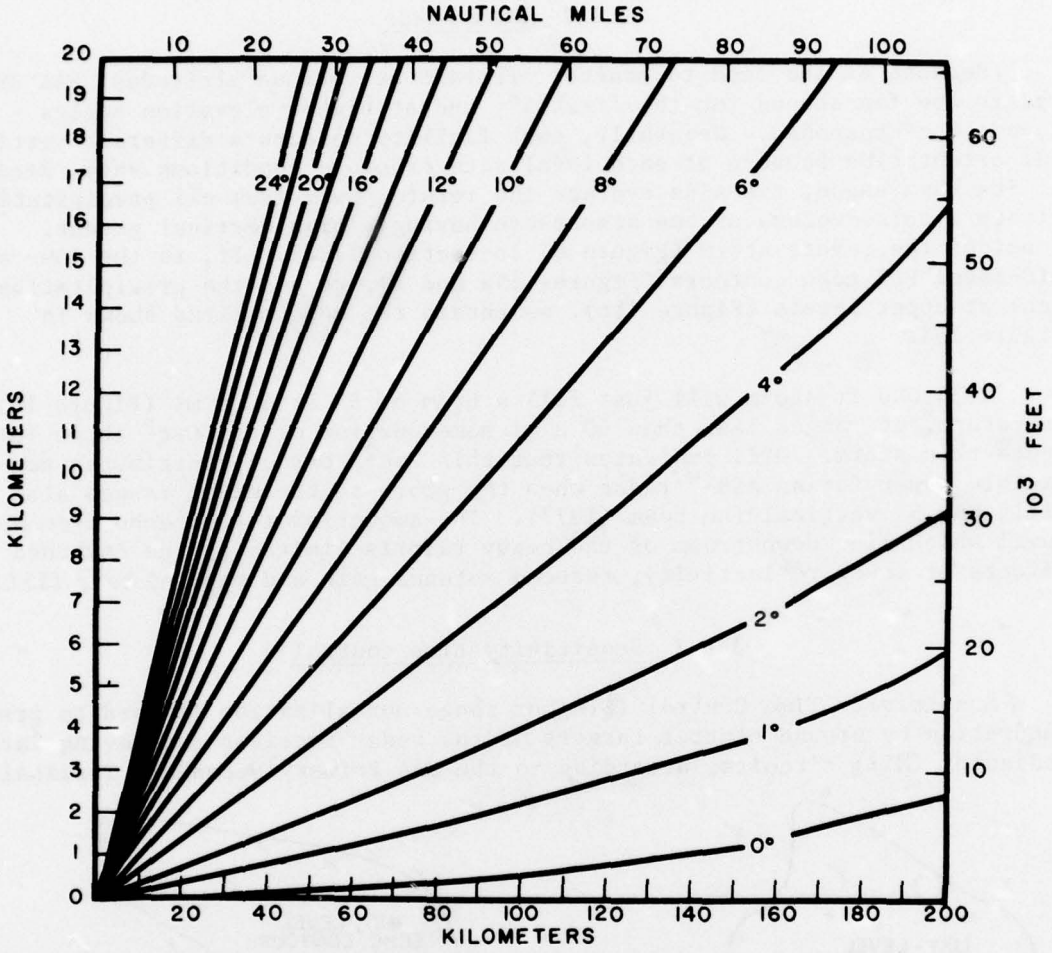

Figure 16. Nomogram of slant range (horizontal axis) versus height above earth (vertical axis) for various elevation angles.

Radar Siting Handbook. Each facility has a choice of selecting the optimum operational STC function in incremental powers from R^1 to R^4 (R^5 on the ASR-8) where R is range. Generally, R^4 is used and is set to start at the edge of the ground clutter, typically 25 n mi. However, the correct STC function for weather that fills the radar beam is R^2. On ASRs, with no STC between 60 n mi and the edge of the ground clutter (~25 n mi) the radar's sensitivity increases as one approaches the radar permitting lighter and lighter precipitation to be detected. Along the leading edge of a squall line where the reflectivity gradients are strongest, the STC may change the shape of the leading edge displayed on the PPI. Also, there is a pronounced change in the displayed maximum echo strength. Figures 17a and 17b compare a squall line with an R^2 STC function to one without STC. Note that echo strength is almost unaffected near the edge of the scope, while the close-in echo shows two more contour levels. (It should be realized that the WSR-57 displayed contours are not calibrated properly when the STC is off.) Inside the ground clutter on ASRs, an R^4 function reduces radar sensitivity very rapidly. On a radar display, echoes would appear to weaken

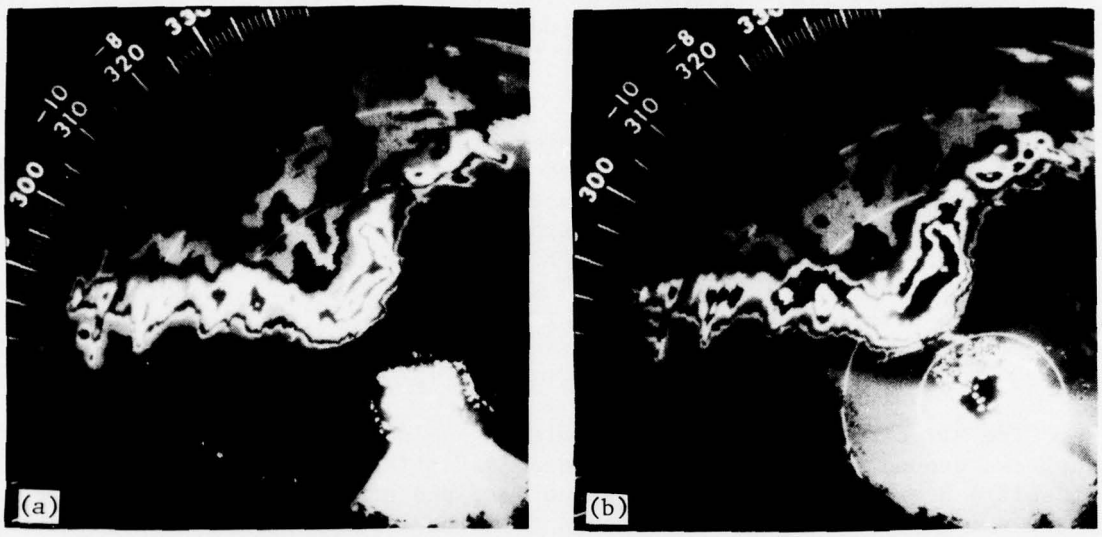

Figure 17. WSR-57 radar PPIs at 2143 and 2144 CST, June 6, 1975, showing a squall line (a) with STC, and (b) without STC. PPI range is 200 km.

and might lose considerable area. Figure 18 shows successive positions of the leading edge of a squall line with exaggerated distortion on an ASR PPI.

3.1.3 Circular polarization

Circular Polarization (CP) is the primary tool used with FAA radars to suppress weather clutter. CP operates on the principle that since precipitation particles are approximately spherical, they return a circularly polarized

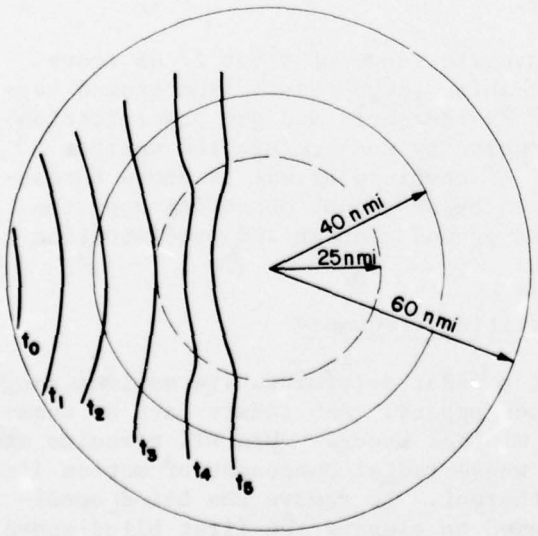

Figure 18. Schematic showing successive positions of a hypothetical squall line's leading edge on an ASR PPI showing curvature due to changes in radar sensitivity as a function of range and STC.

signal essentially unchanged except for reversal of the sense of rotation of the electric field vector, and hence the return is largely suppressed by the antenna. Measurements in rain of actual weather signal losses indicated 12 to 19 dB, independent of reflectivity (Newell et al., 1958; Battan, 1959).

Use of CP when severe thunderstorms are present produces an apparent reduction in total storm area but does not remove the storm entirely. Burnham and Lee (1969) have shown that the presence of severe turbulence in storms (as measured with an F-4C at speeds of 200 to 300 kts) is more likely in more reflective storms but is not necessarily located where reflectivity is strongest. Therefore, this warning: Areas lost by using CP may contain severe turbulence!

3.1.4 Moving target indicator

The MTI ciruits in conjunction with range normalization are used to suppress ground clutter or noise. These establish the phase shift (or lack of shift) between consecutive radar pulses, and stationary targets having no phase shift are subtracted or removed from the radar return. Objects having motion toward or away from the radar do show a phase shift.

In practice, the MTI ciruits suppress echoes with velocities of approximately ±12 kts or greater depending on the velocity response chosen. A velocity notch of finite width is needed to suppress returns from moving clutter (such as leaves and trees blown by wind) and from apparent motion caused by the antenna scanning fixed targets.

When targets (aircraft or precipitation) are moving perpendicularly to the beam, such motion goes undetected because the radial velocity component is near zero. An illustration of this is the display of stratiform rain around the radar location in the form of a butterfly or figure-eight pattern (Figure 19a-e). Even though the stratiform rain has a rather uniform flow, the radial velocity of the rain in directions perpendicular to the flow is zero with respect to the radar.

The MTI circuits have a limited dynamic range of about 27 dB above noise level (Coonley, 1977). If the combined echo return from ground targets and precipitation is below the 27 dB threshold and the precipitation has radial velocities outside the MTI velocity notch, then the weather amplitude remains unaffected. But if the combined signal is above threshold, weather signal amplitude is reduced by an amount depending upon the relative magnitudes of the superimposed ground clutter and precipitation echo returns.

3.1.5 Pulse repetition frequency

The pulse repetition frequency of a radar determines its maximum range before second trip (range folded) echoes appear. ASR radars have an unambiguous maximum range of about 67.5 n mi (833 μsec). When MTI circuits are used, blind speeds exist for aircraft whose radial component of motion lies between 73 and 125 kts and multiples thereof. To remove the blind condition, multiple or staggered PRFs are used to elevate the first blind speed to over 800 kts for ASRs.

(a)

(b)

(c)

(d)

(e)

Figure 19. Sample "figure 8" patterns from NAFEC's ASR-7 radar for (a) 25 dB SCV, (b) 30 dB SCV, (c) 35 dB SCV, (d) 40 dB SCV, and (e) cascade.

Whenever the "false" echoes from storms beyond 67.5 n mi are displayed, they have some shape distortion. While a second trip echo retains its range dimension, its azimuthal extent--or arc length--decreases markedly. Figure 20 illustrates schematically shape distortion from second-time-around echoes with a single PRF. A round echo becomes tear-shaped, but it's possible that a second trip squall line echo could be mistaken for a first trip echo, and many situations will be too complicated for easy identification.

With multiple PRF, a range folded echo is more apparent because it appears as a series of "false" echoes lined up along a common radial. Figure 21 shows range folded echoes from storms on August 10, 1977, in (a) single PRF, and (b) staggered PRF mode.

When MTI is on, "false" echoes are handled the same as first-time around echoes by the velocity notch filter. In addition, the MTI combines the return from three consecutive PRFs so as to minimize signal variance. An echo which otherwise would have a diffuse appearance is filled in. The degree to which an echo is filled in depends on its size, the number of PRFs on the radar and the PRF separation. Second-time-around echoes on ASR-4b, -5, -6 radars, which have have only two PRFs, should always be filled. "False" echoes on the ASR-7 and -8, with six and four PRFs, respectively, may show a diffuse character.

3.1.6 Video gain

Video gain is console controllable and allows the radar operator (air traffic controller) to adjust the voltage level which strikes the scope phosphor and thereby change the brightness of the display. If the gain is set too high, the phosphor saturates and no variation in shading is evident. Furthermore, light from the excited phosphor leaks over adjacent areas and causes fuzziness or blooming. But if the video gain is set too low, weak echoes may be lost and some of these may represent incipient severe development. Therefore, it is a sensible precaution in severe storm situations to adjust the video gain carefully for comprehensive detection.

3.1.7 IF receivers

All ASR radars are provided with linear IF and MTI receivers. In addition, log IF receivers are incorporated into ASR-7 and -8 radars. Linear IF receivers have a usable range of 20 dB and logarithmic IF receivers have an 80 dB dynamic range. In severe thunderstorms, reflectivity usually spans 50 to 60 dB, and when the linear receiver is used, the receiver is saturated over much of the storm, while the log IF receiver rarely saturates. Because of general inability to distinguish showers from thunderstorms with a linear IF receiver, a log IF

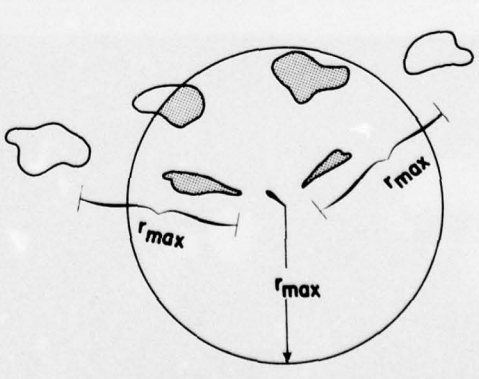

Figure 20, Schematic of sample echo shapes showing distortion to second-time-around echoes from range folding.

(a)

(b)

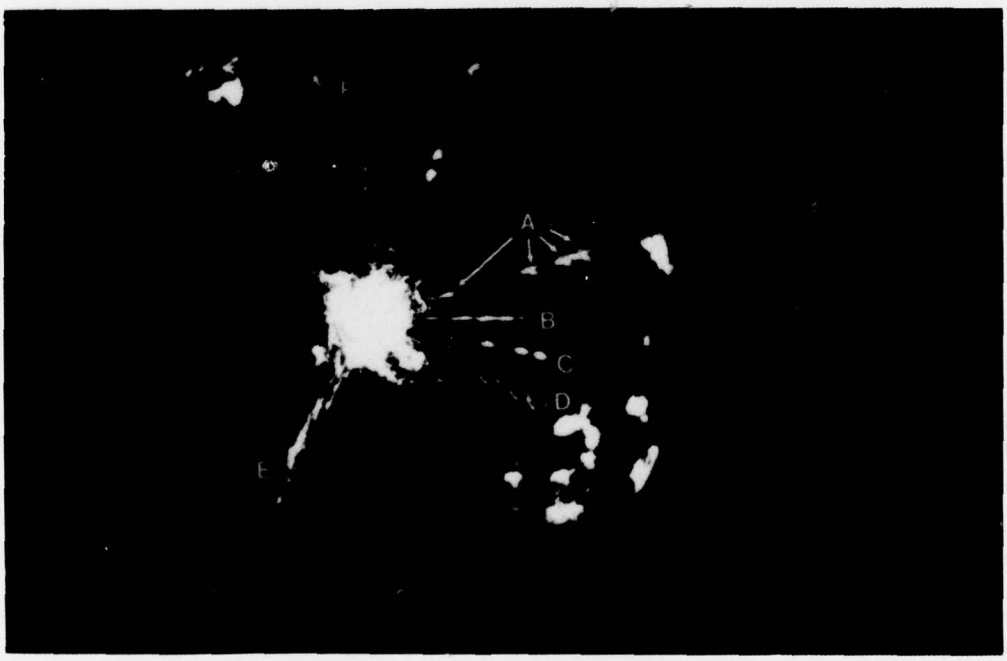

Figure 21. Examples of range-folded echoes on the FAA Academy's ASR-8 radar, August 10, 1977, with (a) single PRF, and (b) multiple PRF.

receiver should be used. ASR radars use a Fast Time Constant (FTC) with the log receiver which cancels the weather echo. On ASR-7 and ASR-8, weather background circuits which contour precipitation areas can be helpful. This type of display, as soon as a storm is determined as severe, can help delineate its boundaries. (Refer to section 3.1.2 for the deleterious effects to weather of the STC set for optimum aircraft detection.)

3.1.8 Low/high beam (ASR-8)

Unlike earlier ASR radars, the ASR-8 has dual feed horns--a normal and a passive one. The high beam passive feed horn is mounted below the primary one. The tilted-up antenna beam is used to decrease the ground clutter. The high beam should also help to increase MTI visibility of weather over ground clutter.

3.2 Applications

3.2.1 Initial scope evaluation

Before proceeding here, the words "storm," "echo," "cell," and "line" need definitions. A storm (or thunderstorm) represents the complete cycle with updrafts, downdrafts, gust fronts, and other manifestations not seen by ASR radars. The echo is restricted to the storm's precipitation. A cell is any defined area of heavy precipitation (maximum return).

A line is defined by the NWS as an area of precipitation whose length is five times or more times its width. The line may be scattered, broken or continuous. Here a line may also mean either a solid squall line or isolated severe storms which are forming on the same discontinuity with gaps of several tens of miles.

In order to determine the degree of organization present the range should be the maximum, since a single isolated severe storm seen on short range may in fact be part of a line! Tornadoes and severe thunderstorms are more likely found in lines or completely isolated large cells than in areas of smaller cells (Bigler, 1955).

Squall lines present a unique problem to scope interpretation. Because of the limited range of 60 n. mi, very often less, the totality of squall lines isn't always seen. In some cases, what may appear as a random pattern may be part of a developing line. Figure 22 compares the same pattern - at full range (100 n mi) and at 60 n mi. Also, with squall lines, the viewing angle of the radar varies appreciably and MTI may cause a significant portion of the line to be substantially attenuated.

Visual clues can be used to separate convective from stratiform systems. The qualitative appearance of stratiform rain is more diffuse and ragged than for convective precipitation, which has a larger ratio of perimeter to area.

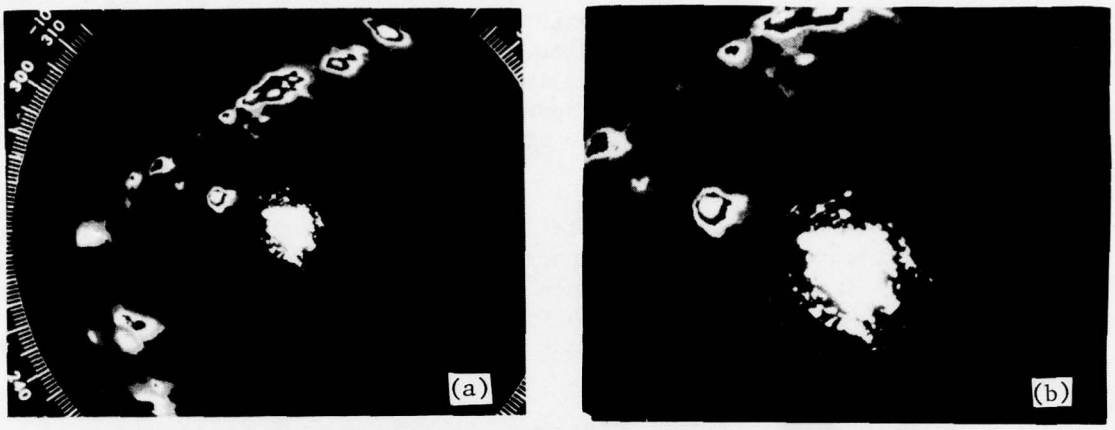

Figure 22. Example of a radar PPI at (a) full range (100 n mi), and (b) clipped at 60 n mi showing loss of information due to range limitation.

Since low level moisture is crucial to severe storms (quoting Lemon, 1977), "...those echoes (storms) which have the least competition for available low level moisture are those most likely to be severe." Those storms that are favorably situated are discussed below.

3.2.2 Isolated echo and squall line characteristics

A. Isolated Storm (especially one ahead of a squall line) or Southern End of a Squall Line: Both have the same favored position with respect to the moisture supply, and hence may be severe. A plane flying through a gap in a squall line is better off staying to the southern edge of the gap (northern edge of storm) unless conditions there are severe. Use of MTI and CP may suppress certain echo areas, thus erroneously displaying the ends and the size of gaps in squall lines.

B. Echo Overhang: An extensive echo aloft often forms on a storm's right flank and slopes downward to the left. Note: This feature is not identifiable on ASR radars since they have no vertical resolution.

C. Bounded Weak Echo Region: Often called a vault or chimney, this is a weakly reflective low-altitude region of a strong updraft that penetrates into the core of the storm beneath the highest echo top. The weak region also is not detected by ASR radar.

D. Hook or Pendant Echo: A hook-shaped echo at low levels wraps around the rotating updraft (Fujita, 1973). Figure 23 shows various configurations. This feature is more easily seen on linear receivers with some attenuation. This kind of hook is detected only at very short ranges by the ASR-8 (<25 n mi) because the radar sees all the vertical extent of a storm beyond 25 n mi. Comparison of CP and linear may facilitate identification of hook echoes in some storms.

Along the leading edge of a squall line the hook is seen as a slight echo protuberance to the north of which is an indentation corresponding to a strong updraft region. Because the winds rotate horizontally within the updraft, it is possible that the MTI circuit could put a zero-velocity notch through the mesocyclone. This depends on the width of the MTI filter, speed of the storm, viewing angle, and strength of the return signal.

E. Strong Reflectivity Gradient: On the right rear quadrant of an isolated severe storm, or the leading edge of a squall line, this feature usually indicates the presence of a strong updraft. It is important to remember, however, that at all ranges, the contribution of echo return from the overhang tends to obscure the reflectivity gradient at low-levels.

F. Flying Eagle or V-Shape: This is another subjective severe storm indicator, presently the subject of some meteorological investigations (Figure 24). This pattern is probably well detected by ASR radars. However, with MTI on, and the radar looking perpendicular to the direction of motion, the V pattern may be lost.

G. Splitting Echoes: A severe storm occasionally divides along an axis perpendicular to storm motion. The left echo, moving much more

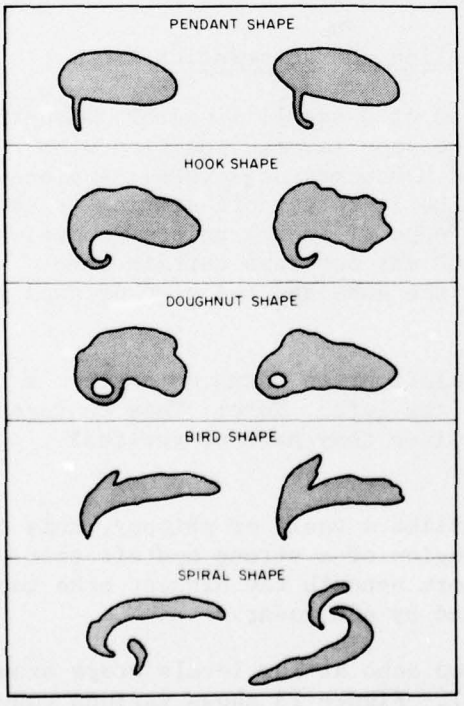

Figure 23. Schematic of various "hook" echo patterns obtained from linear IF receivers. (From Fujita, 1973.)

Figure 24. Example of a "flying eagle" shaped echo from NSSL's WSR-57 radar, April 24, 1975, 2027 CST.

rapidly than the right echo, may have large hail and high winds but not usually tornadoes. The right moving echo may exhibit all three features. Figure 25 shows a sequence for a splitting storm.

Since splitting involves the total storm depth, the phenomenon should be seen under all operating conditions except in special cases where MTI is on.

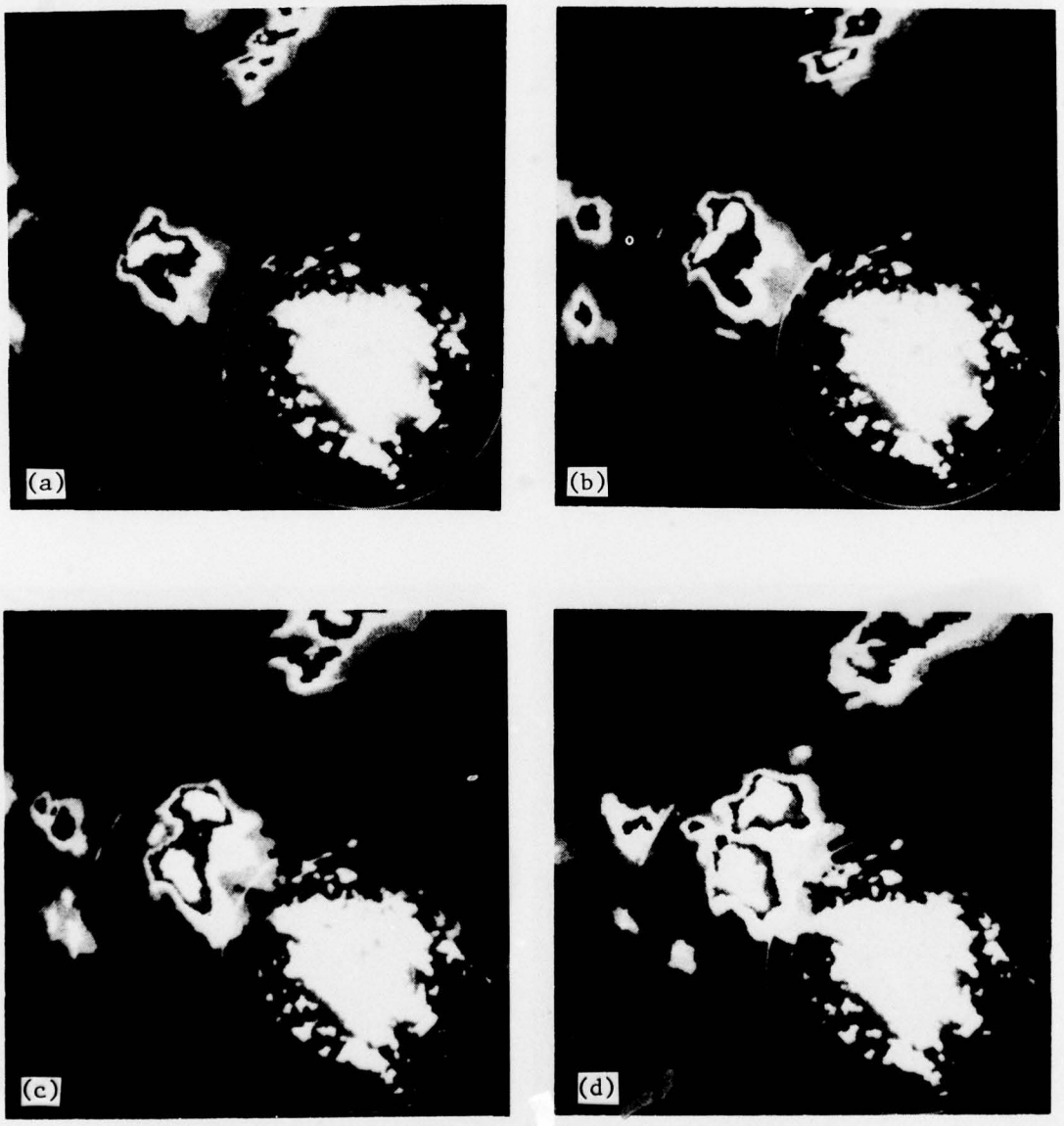

Figure 25. WSR-57 radar PPIs, May 24, 1973, showing a splitting storm sequence at (a) 1509 CST, (b) 1519 CST, (c) 1529 CST, and (d) 1539 CST.

H. Merging Echoes: These may or may not produce severe weather. If a weaker storm merges with a severe storm and obstructs the updraft, the stronger storm may weaken. Only when the merger enhances the updraft region, is severe weather more likely (Figure 26). Other things being favorable, the faster the storms move, the more likely they are to produce severe weather. Also, an echo may merge with a squall line. Merging, too, involves the total storm depth.

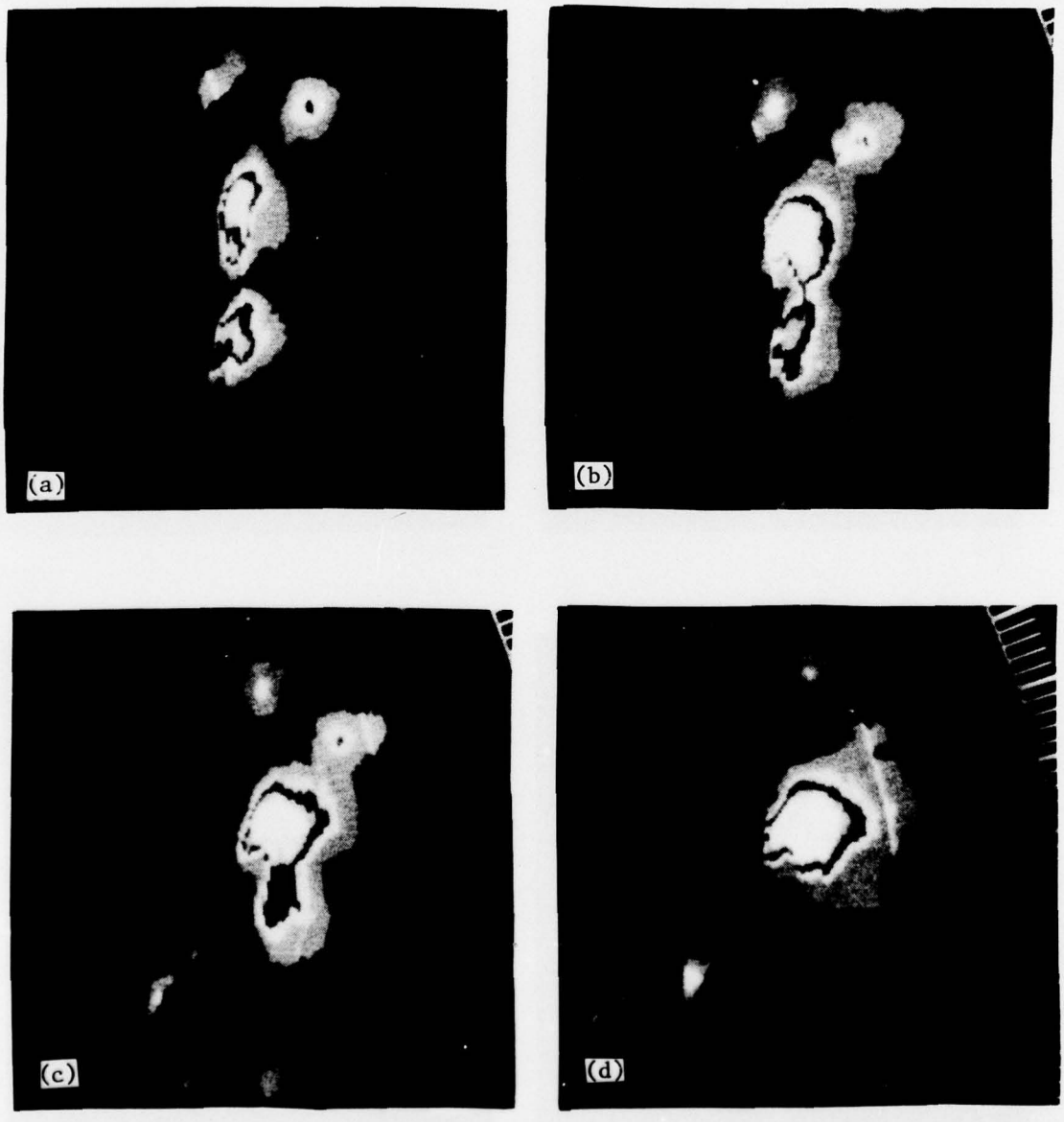

Figure 26. WSR-57 radar PPIs showing merging storms May 6, 1975, at (a) 1409 CST, (b) 1419 CST, (c) 1429 CST, and (d) 1439 CST.

I. Rapidly-Growing Echoes: Storms grow and intensify rapidly because of a strong updraft and frequently have large cores at mid-levels due to the lag in time of falling precipitation. At ranges beyond 25 n mi the ASR's vertical beam (main lobe) helps detect the explosive mid-level growth.

J. Erratic Storm Motion: In large storms, a slowing down or turning to the right may indicate a change from non-severe to severe. Use of STC influences the perception of motion (section 3.1). If this effect is understood, changes in storm motion can be recognized.

K. Storm and Squall Line Motion > 40 kts: Storms or squall lines moving this fast can produce damaging surface winds because the gust front can easily have a combined translational and outflow speed of over 50 kts. These storms may produce large hail and tornadoes.

Speed can be tricky. Although two storms of differing size may be moving at the same speed, the smaller will appear to move faster because it will move the length of itself in a shorter period of time. Also, a large storm may move faster than you think; careful tracking must be maintained.

L. Echo Tops Over 50,000 Ft/Echo Tops 5000 Ft Above Tropopause: Storms in southern Florida in summer regularly can achieve 50,000 ft or higher because there the tropopause is that high. In Florida, in winter, and for the rest of the country, storm tops at 50,000 ft or higher result from a very unstable air mass that permits explosive storm cloud growth and strong vertical air currents. Storms which exceed the tropopause by 5,000 ft or more imply strong updrafts. Also, as explained in Appendix B, storm tops correlate roughly to the maximum reflectivity near the ground. A storm which reaches 50,000 ft corresponds to a storm of about 70 dBZ reflectivity--one almost certain to be severe. Without vertical resolution, ASR radars cannot determine height of storm tops.

M. Line Echo Wave Pattern (LEWP): This feature results when storms form on a bend or wave on a discontinuity, usually the result of cyclogenesis (Nolan, 1959). Stout et al. (1960) found that the line distorted in the direction of line movement and closely corresponded to the areas of most hail and damaging wind. The LEWP shape should be recognized when most of squall line is visible and MTI is off. False LEWP patterns may result if the STC function is R^4 and set at the ground clutter edge.

N. Rotating Squall Lines: Horizontal shear at mid-levels (Fankhauser, 1964) causes differential line motion. Where the winds are strongest, line motion will be fastest. Because it intercepts more low level moisture, this portion is more severe with strong gusty surface winds and a strong gust front likely. Use of STC and MTI may distort or cancel parts of the line; otherwise, the recognizing differential motion depends upon the amount of the line observed.

O. Thin Line/Fine Line: This return is due to density/moisture gradients (and/or insects and birds) or the leading edge of gust fronts. Frequently, new echoes begin on the gust front as it moves away from the parent storm. Fine lines can reach 10 miles from the storm's precipitation (Figure 27).

At very short ranges, STC probably eliminates fine lines, while at longer ranges, the effects of partial beam filling reduce signal strength enough to eliminate their return. Use of CP will guarantee lack of detection while MTI will have the same effect as for squall lines.

Figure 27. WSR-57 radar PPI 2115 CST, June 2, 1971, showing a thin or fine line from a gust front. Range 100 n mi, range marks 20 n mi.

4. SEVERE STORMS OF MARCH 2, 1977

From the FAA Academy ASR-8 radar in Oklahoma City, a sequence of photographs was made of storms which occurred on March 2, 1977. One storm, shortly after photography ceased, produced a tornado near Velma, Oklahoma. This section describes the differences in the photos due to various ASR-8 radar settings.

4.1 Synoptic Situation

The storms of March 2, 1977 were small but were well organized and intense. A strong upper-level low-pressure area developed quickly over the lee slopes of the Rockies, while a surface low formed in central Colorado. Aloft, the air over central Oklahoma diverged and the jet stream axis lay to the west over the Texas and Oklahoma Panhandles. Surface moisture and temperature were near lower limits for severe storms, but surface winds were strong.

4.2 Analysis

About one dozen photographs between 1600 and 1700 CST compare high and low beam, CP, MTI, staggered PRF, and background weather video settings. No STC was used because of time limitations. Scope display range was 60 n mi, range marks at 25 and 50 n mi.

Figure 28a (low beam, single PRF, linear polarization, linear IF gain) shows a continuous line of showers to the northwest and a second, scattered line of thunderstorms, extending southwest from the radar. Figure 28b has the same settings as Figure 28a except that the MTI has been gated to maximum range. Note that because of the difference in viewing angle, more echo was

removed from the line northwest, especially on the southern end, than the line to the southwest. This discrimination suggests that storm motion is to the northeast. Some echo inside the radar's ground clutter has been passed by the MTI.

Figure 28c restored the original radar settings (LP, single PRF, low beam, linear IF). Figure 28d was shot using the radar's high beam at full range; other settings were unchanged. Somewhat unexpectedly, the echo shape remained nearly unchanged. The lack of change indicates that the precipitation formed

(a) Low beam, single PRF, LP, linear IF.

(b) Low beam, single PRF, LP, linear IF, MTI gated to full range.

(c) Low beam, single PRF, LP, linear IF.

(d) High beam at full range, single PRF, LP, linear IF.

Figure 28. PPIs from FAA Academy's ASR-8 radar, March 2, 1977.

from convective processes and had vertical extent. On days with strong winds aloft, precipitation may produce extensive anvil outflow. In Figure 28e circular polarization replaced linear polarization. Because theory suggests that the loss of radar sensitivity due to CP (12-19 dB) is independent of echo strength, we can obtain a measure of storm intensity by comparing the areal changes due to CP of individual echoes. Weak echoes generally have weak gradients while stronger echoes have tighter gradients. Therefore, weak echo regions lose more area when CP is turned on. (Remember that no STC is used here so that sensitivity increases as one approaches the radar.) Figure 28e shows that CP most reduced the area of the echoes closest to the radar, but these echoes were unaffected by high beam. We conclude that these echoes probably are from precipitation falling from the storm anvil. The precipitation northwest was next most affected. Only the northernmost cell retained much of its original area. Also, it has quite uniform shape and brightness. The echoes northwest most likely are thundershowers. Circular polarization least affected the echoes southwest. These echoes are probably thunderstorms whose anvils stretch over the radar site.

Figure 28f was taken using low beam, LP, raw weather video (linear IF), and staggered PRF; MTI was gated to zero range. Use of staggered PRF on March 2, did not show range folded, multiple echo returns as did the examples of August 10, 1977. We conclude that either all the echo is within the range of the radar or, more likely, the echoes which lie beyond 60 n mi have been folded back onto the ground clutter because the two lines of storms do extend to the scope's edge.

(e) High beam at full range, single PRF, CP, linear IF.

(f) Low beam, staggered PRF, LP, linear IF, MTI gated to zero range.

Figure 28. PPIs from FAA Academy's ASR-8 radar, March 2, 1977.

Video from the MTI channel's background weather circuits was photographed in Figure 28g. The background weather video has four modes of operation. Here mode IV, which provides top and bottom clipping of the weather signal, was set at maximum sensitivity. We do not recommend using maximum sensitivity because, as Figure 28g shows, weak signals in the storms' anvils obscure individual storm positions.

Figure 28h shows the maximum suppression achievable on the linear IF weather video (MTI gated to 60 n mi, CP, high beam, staggered PRF). The strongest echoes are still to the southwest. In Figure 28i, MTI was gated to 0 n mi, and single PRF restored. The halo around the ground clutter indicates the video gain was too high. Figure 28j has linear polarization; here the video gain was too low. The last two figures, k and l, show the background video contour combined with the raw linear IF video (only difference is high vs low beam). We don't suggest operating the ASR-8 radar this way because the precipitation would obscure primary aircraft return, but we note the enhanced format of the weather data in these photos.

Figure 29 shows the storms on the WSR-57 radar at the Oklahoma City NWS WSFO for about the same time as Figure 28f. Although the FAA Academy's ASR-8 and the WSR-57 are only separated by about 2 miles, the two pictures differ considerably for at least three reasons: the radar beams have different shapes, the range presented on the WSR-57 is about twice the ASR-8, and the orientation of the ASR-8 is to magnetic north rather than true north.

(g) Low beam, staggered PRF, LP, background weather video mode IV, from MTI channel.

(h) High beam, staggered PRF, CP, linear IF, MTI gated to full range.

Figure 28. PPIs from FAA Academy's ASR-8 radar, March 2, 1977.

The analysis of the storms on this day were strongly biased by a priori knowledge of the severity of the storms. It is doubtful that the same degree of confidence in scope interpretation would have been possible in real time without confirming evidence from the NWS.

(i) High beam, single PRF, CP, linear IF, video gain set too high.

(j) High beam, single PRF, LP, linear IF, video gain set too low.

(k) High beam, single PRF, LP background weather video mode IV from MTI channel.

(l) Low beam, single PRF, LP, background weather video mode IV from MTI channel.

Figure 28. PPIs from FAA Academy's ASR-8 radar, March 2, 1977.

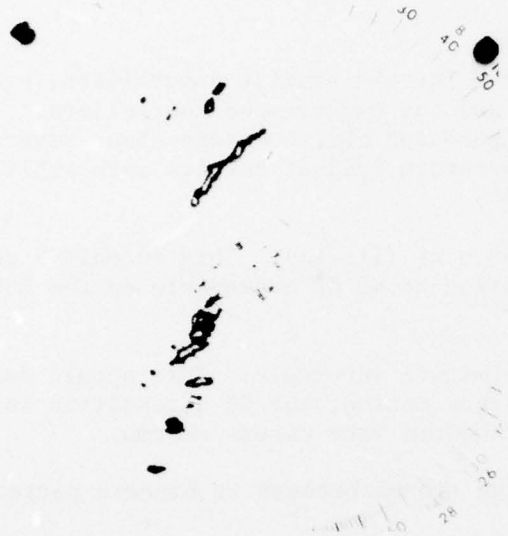

Figure 29. WSR-57 radar PPI from National Weather Service, Oklahoma City, at about 1605 CST.

5. CONCLUSIONS

Effective use of pattern recognition for identifying severe storms comes from training and practice and depends very much on experience. The air traffic controller seldom can practice identifying storms because his first duty, separation of aircraft, demands more of his attention whenever adverse weather is occurring. Moreover, a controller in order to work with traffic uses CP and range-gated MTI circuits which reduce storm signals.

Range normalized weather echo outlines on the ASR-8 when used with special symbols to show core intensity, may give air traffic controllers enough information to decide which storms pilots should avoid. Phase II of this report considers this.

Some specific conclusions:

A. Echo patterns as seen by ASR radars do not alone provide enough information to determine reliably which storms are severe and which are showers. Other information sources, especially intensity data, must supplement the ASR data.

B. Three dimensional structure of echoes, a reliable identifier of severe storms, cannot be obtained because of the broad vertical beam.

C. There exists a national plan for spreading NWS information about severe storm potential and threats, but ATC facilities are not included. Local arrangements, which include autographic writers and perhaps phone lines, do not provide true up-to-the-minute data on storm intensity and motion.

D. On some ASR radars, log FTC circuit removes nearly all precipitation and is recommended only with background weather video circuits.

We recommend:

A. Upgraded (and updated) training for air traffic controllers, every person going into the field, and for experienced controllers. Advances in technology have increased our knowledge about severe thunderstorms since the Thunderstorm Project results were published in 1948.

B. The use of R^2 normalized to 60 n mi (115 km). This is only 5 dB less than the maximum attenuation of 40 dB achievable on the ASR-8 (Figure 30).

C. Use of CP briefly at 10 to 15 minute intervals. This should delineate reflectivity cores and track motion, but CP attenuation is not enough to distinguish thundershowers from severe storms.

D. Not using MTI when interpreting storms because it hinders pattern recognition.

E. Sending parallel data to the ATCs and ARTCC, as well as to the Central Flow Control; transfer of information would be hastened. Also with high speed automated data links (AFOS in the NWS and EFAS for the FAA's flight service stations) transfer of information between groups could be faster, closer to real time.

F. Lowering the PRFs of the ASR radars in order to reduce the problem of second-time-around weather echoes "cluttering" the radar PPI.

The bottom line of every effort to increase each air traffic controller's awareness of severe storms answers the question: How can increased technical knowledge be used? Two flight service stations--Midland, Texas, and Oklahoma City-- for 18 months received real time, remote radar data from Air Route Surveillance radars in an integrated, contoured, VIP format. The radar data proved useful for briefing pilots and suggests a path for future system development.

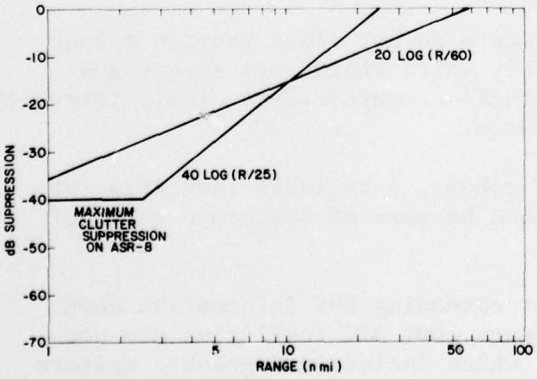

Figure 30. Comparison of R^4 STC function normalized to 25 n mi and R^2 STC function normalized to 60 n mi.

ACKNOWLEDGMENTS

The author wishes especially to thank Mr. Kenneth E. Wilk for his helpful discussions and encouragement during all portions of this work. Messrs. J. T. Lee and Dale Sirmans helped edit this report, and Dr. Edwin Kessler carefully reviewed the work. Mrs. Helen J. Ardrey provided useful insights into the structure and use of language. Mr. Charles Clark and Mrs. Jennifer Moore provided graphic services; Mr. Clark also assisted in photographing the FAA Academy ASR-8 radar. And finally, the author thanks the FAA for funding this work and appreciates their patience in the preparation of this report.

REFERENCES

Barclay, P. A., and K. E. Wilk, 1970: Severe thunderstorm radar echo motion and related weather events hazardous to aviation operation. NOAA Tech. Memo. ERL NSSL-46, 63.

Battan, L. J., 1953: Observations on the formation and spread of precipitation in convective clouds. J. Meteor., 10, 311-324.

Bedard, A. J., Jr., and D. W. Beran, 1977: Detection of gust fronts using surface sensors. NOAA Tech. Memo. ERL WPL-20, 15.

Bigler, S. G., 1955: A comparison of synoptic analysis and composite radar photographs of a cold front and squall line. Proceedings, 5th Weather Radar Conference, AMS, Boston, Mass., 113-119.

Blackmer, R. H., Jr., 1955: The lifetime of small precipitation echoes. Proceedings, 5th Weather Radar Conf., AMS, Boston, Mass., 103-108.

Brandes, E. A., 1973: The variation of Oklahoma spring rains as revealed by radar. Preprints, 8th Conf. on Severe Local Storms, AMS, Boston, Mass., 146-48.

Brandes, E. A., 1977: Gust front evolution and tornado genesis as viewed by Doppler radar. J. Appl. Meteorol., 16, 4, 333-338.

Brown, R. A., D. W. Burgess, J. K. Carter, L. R. Lemon, and D. Sirmans, 1975: NSSL dual-Doppler radar measurements in tornadic storms: A preview. Bull. Am. Meteorol. Soc., 56, 5, 524-526.

Browning, K. A., and D. Atlas, 1965: The initial development of a severe storm as observed by radar. Chapter II, A Family Outbreak of Severe Local Storms - A Comprehensive Study of the Storms in Oklahoma on 26 May 1963. Part I, K. A. Browning Editor. AFCRL, Special Reports, No. 32, 197-236.

Burgess, D. W., and L. R. Lemon, 1976: Union City storm history. Chapter 5, The Union City, Oklahoma Tornado of 24 May 1973. R. A. Brown, Editor, NOAA Tech. Memo. ERL-NSSL-80, 235.

Burnham, J., and J. T. Lee, 1969: Thunderstorm turbulence and its relationship to weather radar echoes. J. of Aircraft, 6, 5, 438-445.

Byers, H. R., and R. R. Braham, 1949: The thunderstorm. U. S. Govt. Printing Office, Washington, D. C., 287.

Charba, J. P., 1977: Two-to-six hour probabilities of thunderstorms and severe weather. Tech. Procedures Bulleting No. 194, Met. Services Div., NWS, NOAA.

Chisholm, A. J., 1973: Alberta hailstorms, Part I: Radar case studies and airflow models. AMS Meteorol. Monographs, 14, 36, 1-36.

Connelly, M.E., 1977: Simulation of transport landings in the presence of wind shear and thunderstorms. Electronic Systems Lab., MIT, ESL-R-744, 64.

Coonley, K., 1977: Personal communication.

Darkow, G. L., 1971: Periodic tornado production by long-lived parent thunderstorms. Preprints, 7th Severe Local Storm Conf., AMS, Boston, Mass., 214-217.

Donaldson, R. J., 1965: Methods for identifying severe thunderstorms by radar: A guide and bibliography. Bull. Am. Meteorol. Soc., 46, 4, 174-193.

Epstein, E. S., 1977: National Severe Local Storms Operation Plan. U. S. Dept. of Commerce, NOAA. Federal Coordinator for Meteorological Services and Supporting Research, 38.

Fankhauser, J. C., 1964: On the motion and predictability of convective systems as related to the upper winds in a case of small turning of wind with height. ESSA Tech. Memo. NSSP-21, 36.

Fawbush, E. J., R. C. Miller and L. G. Starrett, 1951: An empirical method of forecasting tornado development. Bull. Am. Meteorol. Soc., 32, 1, 1-9.

Freund, R. F., 1966: Radar echo signature of tornadoes. Proceedings, 12th Radar Met. Conf., AMS, Boston, Mass., 362-365.

Fujita, T., 1973: Proposed mechanism of tonrado formation from rotating thunderstorm. Preprints, 8th Severe Local Storms Conf., AMS, Boston, Mass., 191-196.

Fulks, J. R., 1951: the instability line. Compendium of Meteorology, AMS, Boston, Mass., 647-652.

George, J. J., Editor, 1960: Weather Forecasting for Aeronautics. Academic Press, New York, N.Y.

Goff, R.C., 1975: Thunderstorm-outflow kinematics and dynamics. NOAA Tech. Mom., ERL NSSL-75. 63.

Golden, J.H., 1974: Life cycle of Florida Keys waterspout, NOAA Tech. Memo., ERL NSSL-70, 147.

Gunn, K.L.S., and T.W.R. East, 1954: The microwave properties of precipitation particles. Quart. J. Royal Met. Soc., 80, 522-545.

Hambidge, R.E., 1967. "K" chart application to thunderstorm forecasts over the western United States. ESSA Western Region Tech. Memo., No. 23, 9.

Kinzer, G. D., 1972: Cloud to ground lightning versus radar reflectivity in Oklahoma thunderstorms. NOAA Tech. Memo., ERL NSSL-59, 24.

Lee, J. T., 1965: Thunderstorm turbulence and radar echoes 1964 data studies. ESSA Tech Note 3: NSSL Report 24, 9-28

Lemon, L. R., 1977: New severe thunderstorm radar identification techniques and warning criteria: A Preliminary Report, NOAA NWS Tech. Memo. NWS NSSFC-1, 58.

Marwitz, J. D., 1972a: The structure and motion of severe hailstorms, Part I: Super cell storms. J. Appl. Meteorol., 11, 166-179.

Marwitz, J. D., 1972b: The structure and motion of severe hailstorms. Part II: Multicell storms. J. Appl. Meteorol., 11, 180-188.

Marwitz, J. D., 1972c: The structure and motion of severe hailstorms. Part III: Severely sheared storms. J. Appl. Meteorol., 11, 189-201.

Mogil, H. M., and H. S. Groper, 1977: NWS's severe local storm warning and disaster preparedness programs. Bull. Am. Meteorol. Soc., 58, 318-329.

Nelson, S. P., 1976: Characteristics of multicell and supercell hailstorms in Oklahoma. Preprints, Int. Conf. on Cloud Physics, AMS, Boston, Mass., 335-340.

Newell, R. E., 1958: A comparison of solid hydrometeor shapes at wavelengths of 3 cm and 5000 A. Proceedings, 7th Weather Radar Conf., AMS, Boston, Mass., 731-737.

Nolen, R. H. 1959: A radar pattern associated with tornadoes. Bull. Am. Meteorol. Soc., 40, 6, 277-279.

Offi, D. L., 1977: Analysis of ATC terminal radar weather detection capabilities. Data Report Activity No. 021-241-120 ATC Systems Div., Surveillance Systems Br., NAFEC, FAA.

Probert-Jones, J. R., 1962: The radar equation in meteorology. Quart. J. Royal Met. Soc., 88, 485-495.

Rasmusson, E.M., 1971: Diurnal variation of summertime thunderstorm activity over the United States. USAF Environmental Tech. App. Center, Tech. Note, 71-4, 12.

Reap, R. M., 1977: Thunderstorm and severe local storm probabilities based on model output statistics--No. 5. Tech. Proc. Bull. No. 199, Met. Services Div., NWS, NOAA.

Reick, R. E., 1977: Teletype radar intensity plot. Tech. Proc. Bull. No. 185, revised, Met. Services Div., NWS, NOAA.

Schaefer, J. T., 1973: The motion and morphology of the dryline. NOAA Tech. Memo., ERL-NSSL-66, 81.

Sharp, W. C., 1976: Primary/secondary terminal radar siting handbook. FAA, Airway Facilities Service, 256.

Sirmans, D., and R. J. Doviak, 1973: Meteorological radar signal intensity plot. NOAA Tech. Memo., ERL NSSL-64.

Skolnik, M. I., 1962: Introduction to Radar Systems. McGraw-Hill, New York, N.Y.

Stout, G. E., R. H. Blackmer, and K. E. Wilk, 1960: Hail studies in Illinois relating to cloud physics. Physics of Precipitation, Geophys. Monogr., 5, Am Geophys. Union Trans., 369-381.

Tegtmeier, S. A., 1974: The role of the surface, subsynoptic, low pressure system in severe weather forecasting. Masters Thesis, Univ. Of Okla., Norman, Okla., 66.

U. S. Weather Bureau, 1947: Thunderstorm rainfall. Hydro-Meteorolgical Rept. No. 5, Part 2. U. S. Dept. of Commerce, U. S. Printing Off., Washington, D. C.

Ward, N. B., K. E. Wilk, and W. C. Herrman, 1965: WSR-57 reflectivity measure measurements and hail observation. ESSA Tech. Note 3, NSSL Tech, Memo. 24, 1-8.

Wilk, K. E., 1976: Evaluation of a remote weather radar display, Vol. 1 - Development and field tests. Report No. FAA-RD-75-60, 37.

Wilk, K. E., J. T. Dooley, and E. Kessler, 1965: Weather detection by ARSR-1D, ASR-4 and WSR-57 radars: A comparative study. Tech. Memo No. 1, NSSL, 33.

Wolford, L. V., 1960: Tornado Occurrences in the United States. Weather Bureau Tech. Paper No. 20 (revised), 71.

Zittel, W. D., 1976: Tall tower measurements preceding the Union City tornadic storm. Chapter 4, The Union City, Oklahoma Tornado of 24 May 1973. R. A. Brown, Editor, NOAA Tech. Memo. ERL-NSSL-80, 235.

APPENDIX A

A1. Radar Equation Applied to Weather Detection

In order to understand the radar return from airplane or weather "clutter" on a PPI scope, it is necessary to discuss mathematically some physical characteristics of the radar beam.

Consider that the sun or a light bulb transmits light in all directions uniformly and thus acts like an isotropic radiator. The light's brightness is proportional inversely to the square of the distance from source $1/R^2$. The brightness or power of a light bulb is measured in watts. A 100-watt light bulb shines twice as brightly as a 50-watt light bulb. Also, radar power is expressed in watts, usually on the order of 500,000. If power shines uniformly in all directions, the power transmitted, P_t, per unit area is $P_t/4\pi R^2$. Even as a flashlight, with a round reflector, concentrates the radar's energy into a narrow beam (directed like a searchlight) so the radar is said to have a gain factor, G. Concentrated radar power per unit area then becomes $P_tG/4\pi R^2$. When the signal arrives at a target, the total energy intercepted depends on target size, σ (called the back-scattering cross section), or $P=P_tG\sigma/4\pi R^2$. Practically, the energy intercepted and returned by an airplane is isotropic and, hence, the returned power P_r varies also as $1/R^2$. The power per unit area at the radar site is $P_t/(4\pi R^2)^2$. Since the same reflector that concentrated the transmitted power also collects the return power, the total power returned to radar depends on the effective collection area of the radar reflector which--from theoretical considerations--we use $Ae = G\lambda^2/4\pi$ where λ is the wavelength of the radiation transmitted by the radar. Substituting, the final equation for the return power from point target is

$$P_r = \frac{P_t G^2 \lambda^2 \sigma}{64\pi^3 R^4} \qquad (1)$$

A useful concept defines the width of the radar beam in terms of its half power points. The shape and size of the radar's reflector determines the antenna pattern. Weather surveillance radars use a parabolic reflector to produce a symmetrical cone-shaped beam which for the WSR-57 weather radar is 2^o (Figure A1). However, the FAA uses a reflector which produces Csc^2-shaped beam. Typical ASR pattern half power points are 5^o in elevation and 1.5^o in azimuth (Figure A2). (Also refer to section 3.1.1 Beam shape.) For some radar parameters of the WSR-57and ASR radars, see Table A1.

An airplane cannot fill a radar beam, but large thunderstorms and squall lines do. (FAA radars have a range limit discussed in section 3.) However, we consider only weather radars whose beam is filled by precipitation targets.

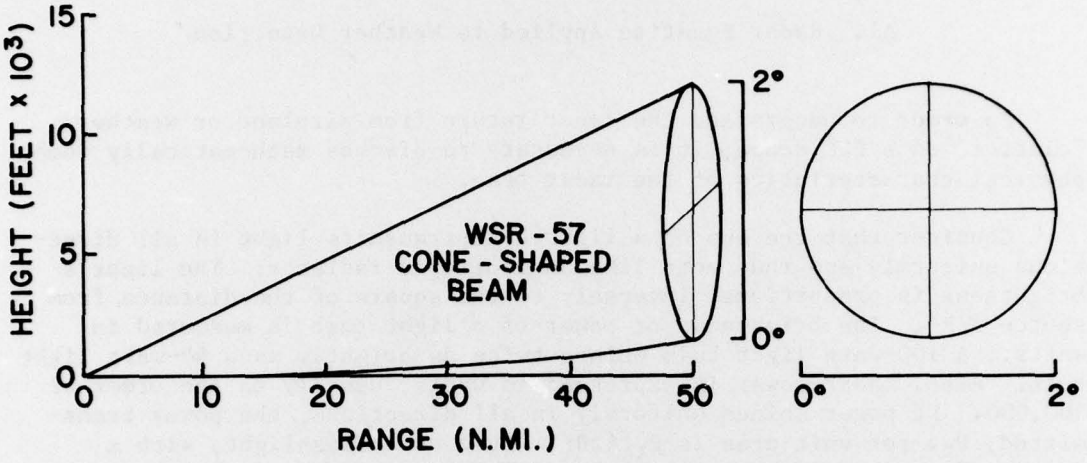

Figure A1. Schematic of WSR-57 cone-shaped beam at the half power points.

A radar sees ensembles of raindrops, hail, snow, or ice crystals as the back-scattering cross section from precipitation. The total back-scattered power depends on the type of precipitation, size of each hydrometeor, radar beam size, and wavelength. Moreover, the radiation, depending on the wavelength can interact in many different ways with hydrometeors. The back-scattering cross section σ for precipitation may be expressed as $\sigma = V_m \Sigma \sigma_i$ (Skolnik, 1962) where σ_i is the cross section of the ith particle and V_m is the volume coverage of the antenna beam defined by the half power beam angles. The volume of a beam is given as

$$V_m = \pi\left(\frac{R\theta}{2}\right)\left(\frac{R\phi}{2}\right)\frac{h}{2} \tag{2}$$

where θ is the horizontal beam width; ϕ, the vertical beam height; and h, pulse length.

Using the Rayleigh approximation to the Mie scattering theory (Gunn and East, 1954) yields

$$\Sigma\sigma_i = \frac{\pi^5}{\lambda^4}\,|K|^2 \Sigma D_i^6 \tag{3}$$

where $|K|^2$ is the complex index of refraction, which for rain has a value of .93. λ is the wavelength of the radar and ΣD_i^6 is the summation of the sixth powers of particle diameters per cubic meter and by convention

Table A1. Comparative Radar Characteristics*

	ASR-4B	ASR-5 & 6	ASR-7	ASR-8	WSR-57
Wavelength	10.3-11.1 cm	10.3-11.1 cm	10.3-11.1 cm	10.3-11.1 cm	10.3-11.1 cm
Peak Power	400 kW	400 kW	400 kW	1 MW	400 kW
Antenna Gain	34 dB	34 dB	34 dB	33.5 dB	38.6 dB
Pulse Length	250 m	250 m	250 m	180 m	1200 m
Minimum Detectable Signal	-109 dBm (Linear IF)	-109 dBm (Linear IF)	-108 dBm (Linear IF)	-110 dBm (Linear IF)	-108 dBm (log IF)
PRF	710-1200 pps	710-1200 pps	710-1200 pps	710-1200 pps	164 pps
Range	60 n mi	60 n mi	60 n mi	60 n mi	300 n mi
Horizontal Beamwidth, θ (half-power points)	1.5°	1.5°	1.5°	≥1.35°	2°
Vertical Beamwidth, $\emptyset$	≈5°	≈5°	≈5°	≥4.8°	2°
Polarization	Vertical and circular	Vertical and circular	Vertical and circular	Vertical and circular	Horizontal

*All ASR characteristics are drawn from the Primary/Secondary Terminal Radar Siting Handbook.

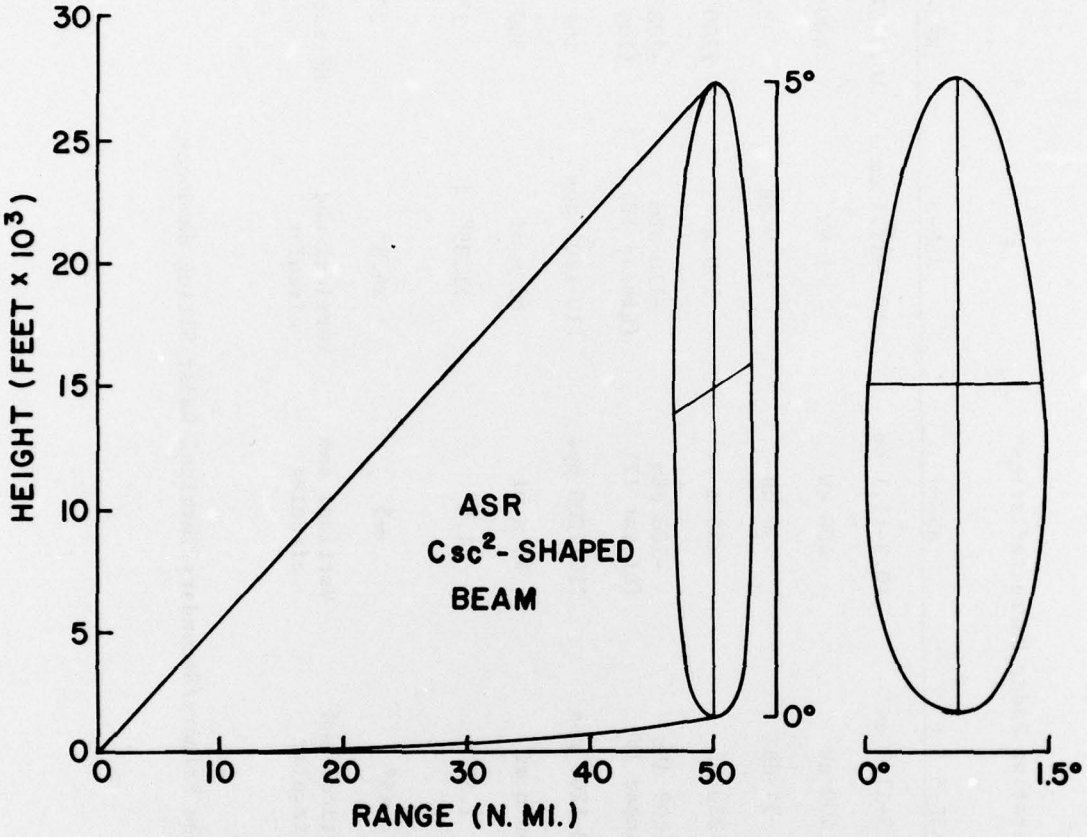

Figure A2. Schematic of typical ASR Csc^2-shaped beam at the half power points.

designated Z, the reflectivity factor. Introducing a correction factor, $2 \log_e 2$ (Probert-Jones, 1962) to approximate the Gaussian power density function for a circular parabolic reflector and combining Eqs. (2) and (3) yields

$$\sigma = \frac{\pi^6 R^2 \theta\phi h |K|^2 Z}{16 \lambda^4 \log_e 2} \quad . \tag{4}$$

Combining Eqs. (1) and (4) yields

$$P_r = \frac{\pi^3 P_t G^2 \theta\phi h |K|^2 Z}{1024 R^2 \lambda^2 \log_e 2} \tag{5}$$

Since radars have fixed basic cahracteristics, almost all our terms can be combined as one value, C, the radar constant. Rewritten, Eq. (5) becomes

$$P_r = \frac{ZCP_t}{R^2} \tag{6}$$

Since the return power to a radar has a wide dynamic range (about 10 orders of magnitude from 10^{-14} to 10^{-4} watts), power is expressed in a common logarithm form as

$$\log_{10} P_r = \log_{10} Z + \log_{10} C + \log_{10} P_t - 2 \log_{10} R \tag{7}$$

Radar people normalize the return signal to a milliwatt and multiply the result by 10 which gives return power expressed as dBm (decibels of power referenced to a milliwatt). Eq. (7) becomes:

$$10 \log \left| \frac{P(\text{Watts})}{10^{-3}} \right| = 10 \log Z + 10 \log C + 10 \log P_t - 20 \log R + 30 \ . \tag{8}$$

Expressing the reflectivity factor, Z, in decibels yields:

$$dBm = dBZ + 10 \log C + 10 \log P_t - 20 \log R + 30 \tag{9}$$

where 30 is 10 log 10^3, the conversion from watts to milliwatts. Meteorologists are interested in dBZ. When the terms are rearranged, Eq. (9) becomes

$$dBZ = 20 \log R - 30 + dBm - 10 \log C - 10 \log P_t. \tag{10}$$

Every radar has a minimum detectable signal, MDS, below which a return signal cannot be distinguished from background thermal noise. The MDS in decibels is -108 for the WSR-57, -110 for the ASR-8*, and -109 for the ASR-4 through 7. From Eq. (10), minimum detectable dBZ varies as a function of range for any given radar, and that a comparison of different radars' ability to see weather is the computed minimum detectable dBZ for each radar at the same range. Table A2 gives minimum detectable dBZ values for each radar at 60 n mi; the lower dBZ value indicates the more sensitive radar.

In actual practice we don't allow a radar's sensitivity to weather (precipitation) to vary with range. The reason for constant sensitivity: as phenomena such as severe storms approach, the echo would seem to grow larger and more intense and, conversely, as storms move away they would appear to grow smaller and weaker.

To get constant sensitivity, range normalization or sensitivity timing control (STC) is used on weather radars. The usable range is declared (for the WSR-57, 125 n mi) and the return signal is attenuated in a controlled manner beginning at that range as a storm approaches the radar. If we compare Eq. (1) to Eq. (5), we see that the denominator of the first equation has R^4, while

---

*Log normal video

Table A2. ASR and WSR-57 Sensitivity Comparison at 60 n mi.

Radar	Radar Constant (C)	dBZ (Minimum Detectable)	Equivalent Rain Rate (in/hr)
ASR-4B	3.73×10^{-18}	14.86	.0122
ASR-5,6	3.73×10^{-18}	14.86	.0122
ASR-7	3.73×10^{-18}	14.86	.0122
ASR-8	1.84×10^{-18}	12.90	.0092
WSR-57	7.94×10^{-17}	3.76	.0021

Eq. (5) has the term R^2. Because the radar beam is filled (we assume with precipitation) the volume of the return energy increases in proportion to R^2. Therefore, if reflectivity from precipitation is uniform, the average echo power received from a distributed target falls off with the inverse square of the range. Typically, FAA radars are range normalized for $1/R^4$ while weather radars are range normalized for $1/R^2$. (Refer to section 3.1.2, Sensitivity time control, for effects of optimum STC on display of weather echoes.)

Because return echo from precipitation is due to many hydrometeors, the signal strength fluctuates over several dB from pulse to pulse. In order to smooth the storm presentation on a PPI scope, several pulses over a small region are averaged. Theory shows that 31 statistically independent samples are needed to reduce signal variance to about 1 dB (Sirmans and Doviak, 1973).

A2. Rainfall Rate Related to dBZ

Over the last 20 years, many and various investigators conducted experiments to find empirically what relationship exists between rainfall rate and the reflectivity factor Z. The formula frequently cited now is the Marshall-Palmer relationship:

$$Z = 200\ R^{1.6} \tag{11}$$

where R is the rainfall rate in millimeters per hour. By expressing the reflectivity factor in terms of dBZ and solving for R, yields

$$R = 10^{\frac{dBZ-23.01}{16}} \tag{12}$$

This relationship assumes a uniform distribution of raindrop sizes and that there is no hail present--not a good assumption for severe storms! Table A3 shows the rainfall rates mm/hr and in/hr obtained for different dBZ values.

Table A3. Rainfall Rates for Different dBZ Values.

	Rainfall	
dBZ	mm/hr	in/hr
10	0.15	.006
20	0.65	0.03
30	2.73	0.11
40	11.5	0.45
50	48.6	1.91
60	205.0	8.07
70	865.0	34.04

APPENDIX B

Relationships Between Storm Reflectivity and Severe Weather Events

The relationship between displayed contours of intensity and severe weather events was defined from studies at NSSL and elsewhere, expressed in statistical probabilities. Similar criteria are used also by the NWS in severe storm diagnosis and issuance of warnings.

Figure B1 shows hail (distribution of Oklahoma hail was reported by volunteer observers) in relation to thunderstorm intensities as observed with NSSL radar (Ward et al., 1965). Please note that about 85 percent of the hail producing storms are identified by intensities stronger than 50 dBZ. In a small fraction of cases with intensities less than 50 dBZ, 73 percent of hail diameters averaged 1/4 inch or less. With intensities less than 40 dBZ, hail is rare and small. At this time, we are not able to say with certainty what percentage of echoes of a specified intensity contains hail; only when hail is reported, peak storm reflectivities usually are higher than 50 dBZ. Of course, in the tropics storms do produce rainfall rates with comparable reflectivities, without hail. And so radar measurements in warm coastal states may require more meteorology information for proper interpretation.

Freund related 13 tornadic storms that occurred in 1964 - between 20 and 100 n mi of NSSL - to their radar echo signatures. Apparent hook echoes were observed in six cases. In all but one case, echoes were at least as reflective as thunderstorms producing small hail. But no single feature appears on the WSR-57 radar to distinguish clearly the echoes from other cellular rainstorms producing small hail.

An example of dual-Doppler wind fields and the simultaneous contouring of reflectivity pattern by the WSR-57 is shown in Figure B2. Figure B2a shows two single-Doppler velocity fields combined into relative horizontal wind vectors at grid points spaced 2.5 km apart (Brown et al., 1975). The vectors are superimposed on a radar reflectivity field derived from measurements at the two Doppler radars. Figure B2b presents the WSR-57 contoured

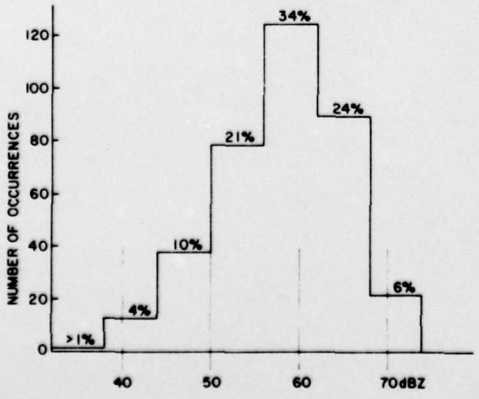

Figure B1. Distribution of Oklahoma hail occurrences in relation to the maximum radar reflectivity of storm cores. (From Ward et al., 1965.)

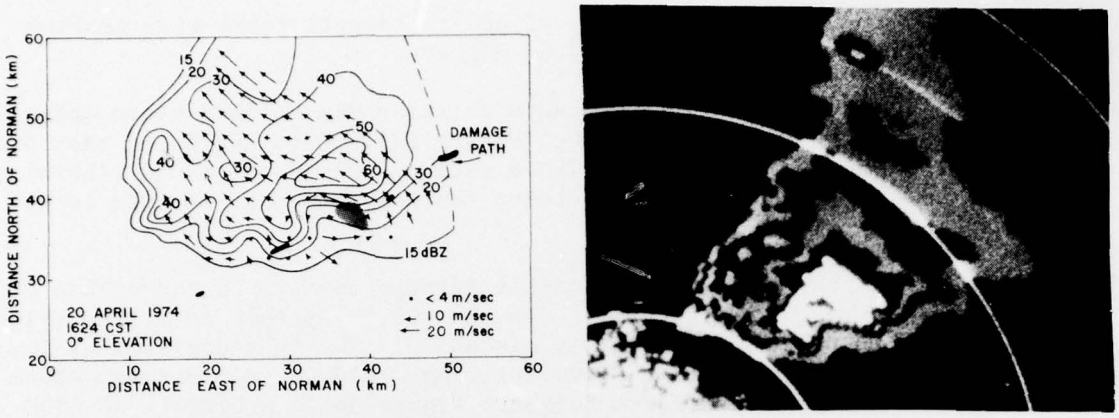

Figure B2. NSSL dual-Doppler wind fields and WSR-57 display: (a) horizontal wind field (relative to the storm) at a height of 0.2 km deduced from the NSSL dual-Doppler system, (b) the WSR-57 contoured display for the same time. (From Brown et al., 1975.)

display for the same time. There is general southeasterly flow through the storm at this low altitude with a noteworthy region of non-uniform cyclonic circulation bounded on the west by a curved reflectivity pattern. This is the first dual-Doppler radar confirmation whose cyclonic curvature suggests the hook echo reflectivity pattern (Figure B2b) and is a sign of mesoscale cyclonic circulation. The storm caused intermittent surface tornado damage (broad line segments). The darker stippled region at 38 km east, 38 km north, indicates an area where both radars measured Doppler spectrum variances so large that reliable mean velocity values could not be determined. However, large variances signify strong velocity gradients within the radar beam width.

A relationship exists between maximum storm intensity and categories of turbulence (Figure B3, Burnham and Lee, 1969). Intensity and turbulence were compared using parameters from the instrumented aircraft and concurrent intensity data from the WSR-57 radar. Lee (1965) concluded that the storm maximum reflectivity was still the most reliable indicator of turbulence, and that

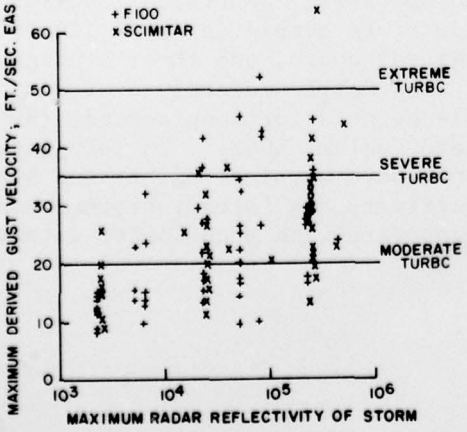

Figure B3. Maximum storm intensity and maximum derived gust velocities and categories of turbulence (Burnham and Lee, 1969.) EAS is the equivalent air speed.

severe turbulence is almost wholly confined to target storms with maximum radar reflectivity, Z_e, of $10^4 mm^6 m^{-3}$ or higher.

Kinzer's study (1972) established a relationship between storm intensity and cloud-to-ground lightning flashes (Figure B4). Data suggested that areas of stronger reflectivity may have higher rates of cloud-to-ground lightning flashes. The formative mechanics between thunderstorms and sferics is not settled.

An organized squall line can contain intense centers of convection (Figure B5, Barclay and Wilk, 1970). As the WSR-57 antenna is tilted (Figure B5c), storm echo cores are easily discerned. The juxtaposition of low level storm centers to the tops shows the close relationship between storm intensity at low levels and storm height. Figure B6 is a summary of 7000 measurements of low level (0.5° tilt) individual thunderstorm intensities and their associated tops. These data were made with 29 NWS WSR-57 radars and represent all types of convective activity (e.g., air mass, frontal, squall lines, etc.) extending from southern Florida to Canada. Because observations were made with a linear response receiver and an A-scope display, the estimated intensity values are higher than the true averaged power by some 6 dB. Corrected for this offset, the expected radar echo heights with maximum reflectivities of 30, 40, 50, and 60 dBZ, fall about 25, 35, 42, and 47 thousand feet. The first standard deviation of the mean height is 5400 ft. Since in 1953 Battan decided the vertical growth period of individual echoes is about 20 to 30 minutes, and that average cell lifetime is 40 minutes (Blackmer, 1955), probably most hourly reports of echo tops are uncorrelated. Furthermore, error, so common in extrapolation, may be even higher in estimating the echo top from the low level reflectivity. Of course, cell 'conglomerates," generally labelled thunderstorm complexes, have lifetimes of several hours, and their average cell tops may be maintained at considerable heights for long periods (Browning and Ludlam, 1962). In long lasting storms, both vertical extent and high reflectivity are 'steady state,' and commensurate with much longer intervals.

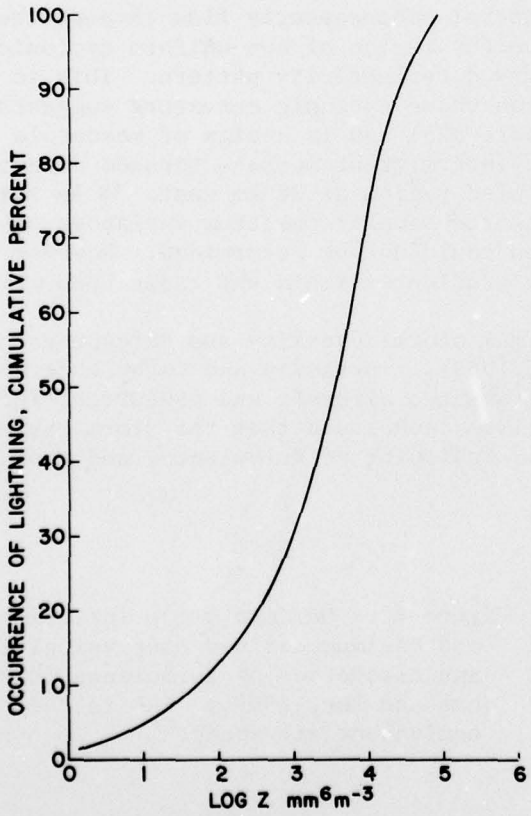

Figure B4. Storm intensity and the occurrence of cloud-to-ground lightning (Kinzer, 1972).

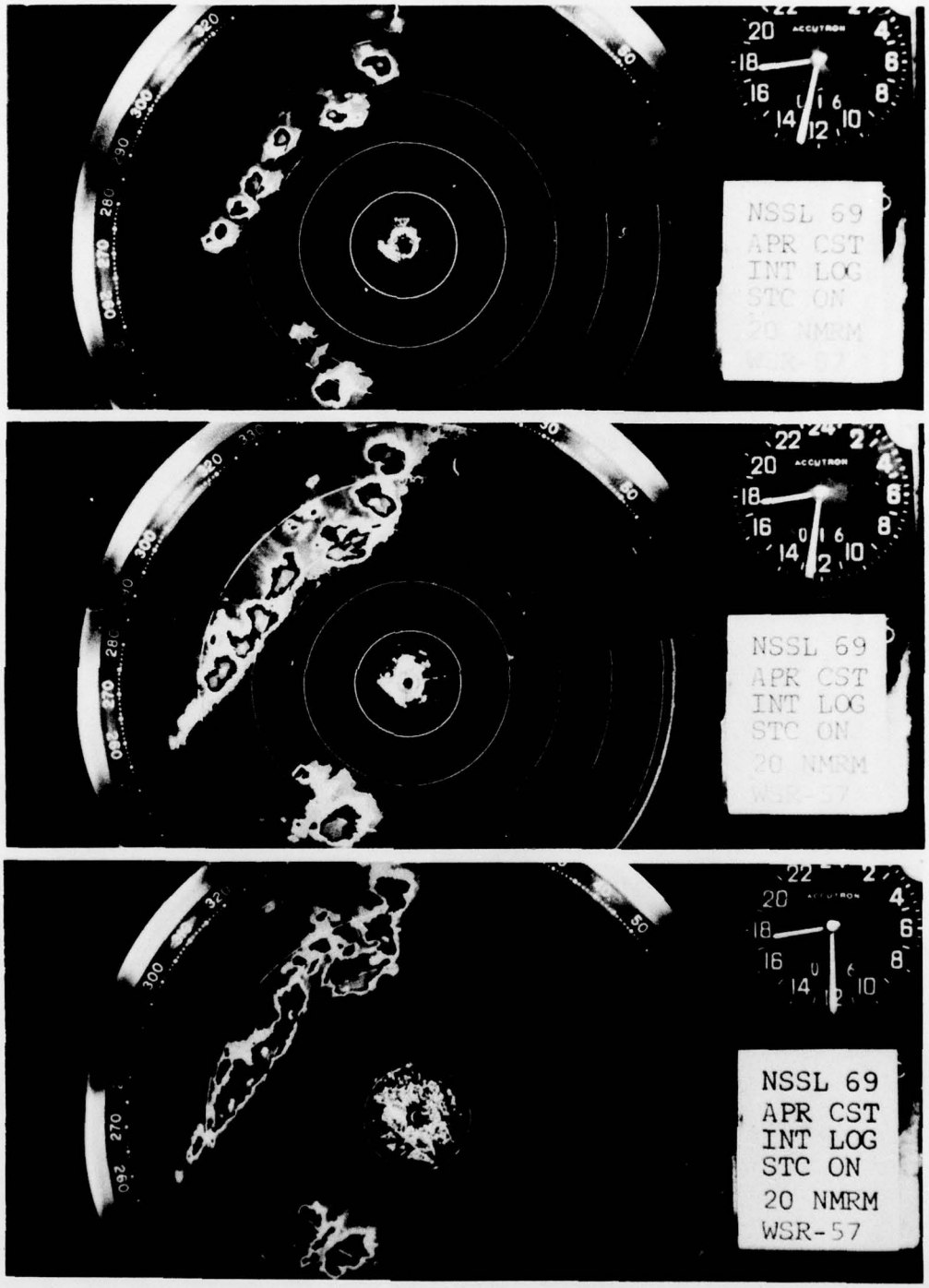

Figure B5. WSR-57 radar contoured 100 n mi display for April 16, 1969. The first intensity level, 10 dBZ, bright cores 50 dBZ. (a) antenna tilt is zero degrees, (b) antenna tilt is one degree, and (c) antenna tilt is two degrees. Range is 100 n mi, range marks at 20 n mi intervals.

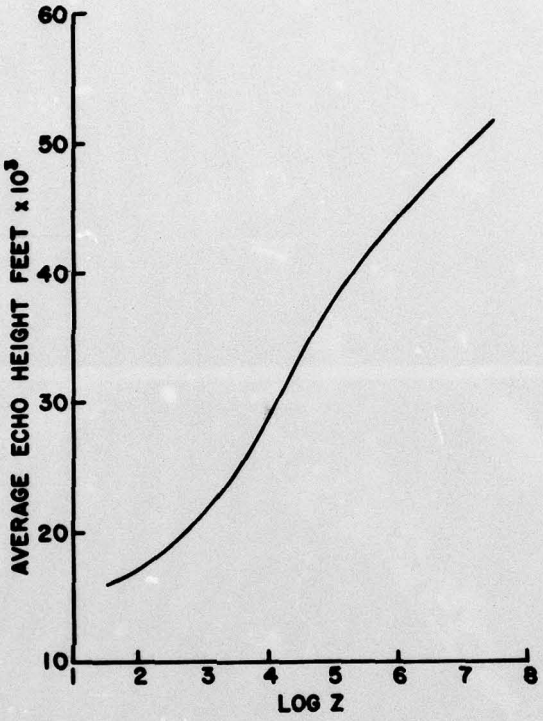

Figure B6. A summary of 7000 measurements of low level (0.5° tilt) individual thunderstorm intensities and their associated tops.